



Cite this: *RSC Chem. Biol.*, 2023, 4, 533

## P<sub>1</sub> Glutamine isosteres in the design of inhibitors of 3C/3CL protease of human viruses of the *Pisoniviricetes* class

Louise A. Stubbing,<sup>ab</sup> Jonathan G. Hubert,<sup>a</sup> Joseph Bell-Tyrrer,<sup>a</sup> Yann O. Hermant,<sup>ID ab</sup> Sung Hyun Yang,<sup>a</sup> Alice M. McSweeney,<sup>bc</sup> Geena M. McKenzie-Goldsmith,<sup>bc</sup> Vernon K. Ward,<sup>ID bc</sup> Daniel P. Furkert<sup>ID ab</sup> and Margaret A. Brimble<sup>ID \*ab</sup>

Viral infections are one of the leading causes of acute morbidity in humans and much endeavour has been made by the synthetic community for the development of drugs to treat associated diseases. Peptide-based enzyme inhibitors, usually short sequences of three or four residues, are one of the classes of compounds currently under development for enhancement of their activity and pharmaceutical properties. This review reports the advances made in the design of inhibitors targeting the family of highly conserved viral proteases 3C/3CL<sup>PRO</sup>, which play a key role in viral replication and present minimal homology with mammalian proteases. Particular focus is put on the reported development of P<sub>1</sub> glutamine isosteres to generate potent inhibitors mimicking the natural substrate sequence at the site of recognition.<sup>1</sup>

Received 25th May 2023,  
Accepted 19th June 2023

DOI: 10.1039/d3cb00075c

rsc.li/rsc-chembio

### Introduction

The *Pisoniviricetes* class encompasses a diverse range of positive-sense single-stranded RNA viruses infecting eukaryotic organisms. Importantly to humans, this class includes the *Picornaviridae*, *Coronaviridae* and *Caliciviridae* families which represent some of the leading causes of acute morbidity in humans,<sup>1</sup> and are among the most prevalent infectious agents. Picornaviruses are a large family of viruses, infecting both humans and animals, and their pathology ranges from mild infections such as the common cold and hepatitis A to more severe disease including meningitis and paralysis. In some instances viral infections by picornaviruses have been linked to autoimmune diseases such as myocarditis, diabetes, and multiple sclerosis.<sup>2–6</sup> Coronavirus infections also span a range of severity,<sup>2,7</sup> while caliciviruses are the leading cause of acute gastroenteritis but can have more severe symptoms in immunocompromised individuals.<sup>8</sup> One of the unifying features of the *Pisoniviricetes* class is a highly structurally conserved cysteine protease belonging to the PA clan (proteases of mixed nucleophile,

superfamily A), commonly referred to as 3C<sup>PRO</sup> (picornaviruses) or 3CL<sup>PRO</sup> (coronaviruses and caliciviruses, also known as M<sup>PRO</sup>). 3C<sup>PRO</sup> and 3CL<sup>PRO</sup> enzymes play a critical role in viral replication, initially catalysing their autocleavage from the nascent polypeptide chain, before performing secondary cleavages leading to maturation of the viral replication machinery.<sup>9–11</sup>

3C<sup>PRO</sup> and 3CL<sup>PRO</sup> are chymotrypsin-like cysteine proteases, which have characteristic folding of two equivalent  $\beta$ -barrels to form the binding pocket and a catalytic triad or dyad.<sup>12–14</sup> Substrate recognition is typically dictated by a hexapeptide sequence (P<sub>4</sub>–P<sub>3</sub>–P<sub>2</sub>–P<sub>1</sub>–P<sub>1'</sub>–P<sub>2'</sub>), each amino acid interacting with its corresponding binding site (S<sub>x</sub>) of the protease enzyme (Fig. 1A). The scissile bond is between the P<sub>1</sub>–P<sub>1'</sub> residues which are typically glutamine (Gln)–glycine (Gly), or Gln–other small amino acid. Though cleavage occurs less commonly, glutamic acid (Glu)–glycine (Gly) is another peptide bond of interest.<sup>15,16</sup> Crystal structures of 3C<sup>PRO</sup> and 3CL<sup>PRO</sup> proteases along with substrate specificity studies have demonstrated subtle variation in the binding pockets and orientation of the catalytic triad/dyad, however all are remarkably conserved to recognise glutamine at P<sub>1</sub> position. Specificity for P<sub>1</sub> glutamine is attributed to conserved histidine (His) residue located at the end of the S<sub>1</sub> binding pocket which form important hydrogen bonds with the glutamine side chain of the natural substrate. Due to the critical roles that 3C and 3CL<sup>PRO</sup> play in viral replication and minimal homology with mammalian proteases, 3C<sup>PRO</sup> and 3CL<sup>PRO</sup> have emerged as promising targets for drug

<sup>a</sup> School of Chemical Sciences, The University of Auckland, 23 Symonds Street and 3b Symonds Street, Auckland 1142, New Zealand.

E-mail: m.brimble@auckland.ac.nz

<sup>b</sup> Maurice Wilkins Centre for Molecular Biodiscovery, The University of Auckland, 3b Symonds Street, Auckland 1142, New Zealand

<sup>c</sup> Department of Microbiology and Immunology, School of Biomedical Sciences, University of Otago, PO Box 56, 720 Cumberland Street, Dunedin 9054, New Zealand



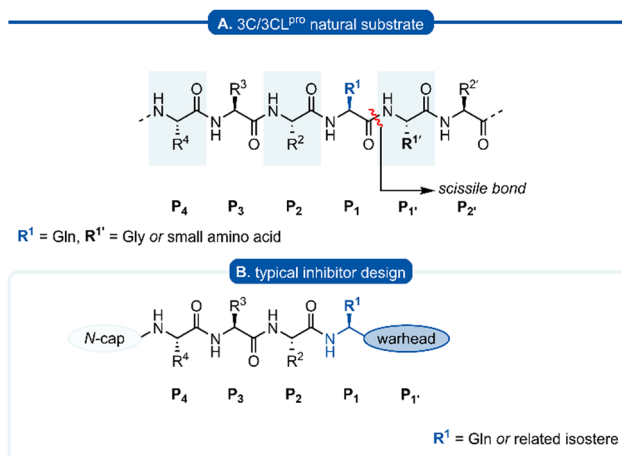


Fig. 1 (A) Hexapeptide recognition sequence of  $3C/3CL^{pro}$ , where the scissile bond is located between  $P_1$  (Gln) and  $P_1'$ . (B) Typical inhibitor design targeting  $3C/3CL^{pro}$ .

development. A commonly employed approach in developing  $3C/3CL^{pro}$  inhibitors is to mimic the natural substrate sequence, replacing the scissile bond with an electrophilic warhead to capture the catalytic cysteine residue, either *via* a reversible or irreversible mechanism. Peptidyl inhibitors targeting  $3C/3CL^{pro}$  typically consist of a two to four peptide sequence ( $P_4-P_1$ ), with glutamine occupying the  $P_1$  position and an electrophilic “warhead” at  $P_1'$  while the N-terminal is protected (N-cap) (Fig. 1B).

Following this blueprint, a number of low micromolar inhibitors targeting  $3C/3CL^{pro}$  have been developed (representative examples, Fig. 2),<sup>17–26</sup> equipped with various electrophilic warheads demonstrating their effectiveness at trapping the catalytic cysteine residue. A drawback of employing a  $P_1$  glutamine residue, however, is the high propensity for the amide side chain (Scheme 1A) to cyclise onto the electrophilic warhead, forming the hemiaminal tautomer (Scheme 1B). This reactivity has been observed with aldehyde,<sup>17,27</sup>  $\alpha$ -haloketone,<sup>23,28</sup> and acyloxymethyl ketone<sup>25</sup> warheads containing  $P_1$  glutamine or  $N$ -monoalkylated glutamine isosteres (see Section 1). Although the effects of tautomerisation to the hemiaminal are not clearly delineated, this is generally considered to be detrimental to antiviral activity while also causing complications during the chemical synthesis and purification. To avoid complications caused by the  $P_1$  glutamine residue in the design of  $3C/3CL^{pro}$  inhibitors, incorporation of a glutamine isostere which binds specifically in the  $S_1$  pocket while also preventing cyclisation onto the electrophilic warhead is desirable. This review reports the advances made in the design of inhibitors targeting viral  $3C/3CL^{pro}$  of human viruses in the *Pisoniviricetes* class and focusses on the reported development of  $P_1$  glutamine isosteres.

## Section 1. $P_1$ $N$ -alkyl glutamine inhibitors

Early work in the development of  $P_1$  glutamine isosteres focused on alkylation of the glutamine side chain amide to retard its nucleophilicity and prevent cyclisation onto the electrophilic warhead. Selected examples of inhibitors possessing

a mono- or di-substituted amide side-chain at  $P_1$  position and equipped with various warhead units are presented in Fig. 3. Malcolm *et al.* explored tetrapeptide inhibitors with  $N,N$ -dimethyl-Gln at the  $P_1$  position.<sup>29</sup>

This was proposed to prevent cyclisation onto the aldehyde warhead while also maintaining hydrogen bonding between the glutamine  $\delta$ -carbonyl oxygen and His<sub>160</sub> of hepatitis A virus (HAV)  $3C^{pro}$ .<sup>12,29</sup> Inhibitor **1a** was based on the preferred substrate sequence and was found to be a reversible, slow binding inhibitor of HAV  $3C^{pro}$ , while also being 50-fold less active against human rhinovirus (HRV)  $3C^{pro}$ . Investigation of a series of  $P_1$  glutaminal inhibitors targeting HRV found  $N,N$ -dimethyl-Gln containing inhibitor **2b** was  $\sim$  50-fold more active compared with the corresponding  $P_1$  glutamine analogue **2a**.<sup>27</sup> The low potency of **2a** was postulated to be due to the propensity for cyclisation to the less active hemiaminal tautomer (see Scheme 1). A similar study was conducted investigating Michael acceptor tetrapeptides for anti-HRV activity. In this study however, unmodified glutamine inhibitor **3a** was found to have superior activity ( $EC_{50} = 0.54 \mu\text{M}$ ) compared with both  $N$ -methyl-Gln **3b** and  $N,N$ -dimethyl-Gln **3c** containing analogues ( $EC_{50} = 5.6 \mu\text{M}$  and  $4.0 \mu\text{M}$ , respectively).<sup>19</sup> The discrepancies in these studies likely arise from the propensity of the unprotected glutamine side chain to cyclise onto the aldehyde warhead, while Michael acceptors have not been observed to undergo cyclisation with the  $P_1$  glutamine residue.<sup>18</sup> A related series of  $N$ -alkylated glutaminal inhibitors, cyclic tertiary amide exemplified by **4** were also shown to be effective in targeting norovirus (NV)  $3CL^{pro}$ .<sup>30</sup>

A glutamine  $N$ -alkylation strategy has also been employed to generate inhibitors equipped with an  $\alpha$ -fluoromethyl ketone (FMK) warhead and targeting HAV<sup>31</sup> and severe acute respiratory syndrome coronavirus (SARS-CoV)<sup>23,28,32</sup>. Compound **1b** was found to inhibit HAV  $3C^{pro}$  and displayed a second order rate constant of  $k_{\text{obs}}/[I] = 3.3 \times 10^2 \text{ M}^{-1} \text{ s}^{-1}$ <sup>31</sup> while  $N,N$ -dimethyl-Gln analogue **5a** was shown to be a low micromolar inhibitor of SARS-CoV replication.<sup>28</sup> The analogous inhibitor **5b** containing an unmodified Gln-FMK unit was found to be predominantly cyclised in solution (as observed by  $^1\text{H}$  NMR) and 200-fold less active against SARS-CoV in a National Institute of Allergy and Infectious Diseases (NIAID) screen. An inhibitor containing an  $N$ -methyl-Gln-FMK unit **5c** was on the other hand reported as active according to a personal communication in a footnote; however partial cyclisation in solution was observed by  $^1\text{H}$  NMR and a series containing this  $N$ -methyl-Gln-FMK unit does not appear to have been pursued further. A series of glutamine-trifluoromethyl ketone inhibitors, represented by inhibitor **6a** ( $K_i > 1000 \mu\text{M}$ ), were all found to be at least partially cyclised in solution (as determined by  $^{19}\text{F}$  NMR in  $\text{CDCl}_3$ ), while some existed solely in their cyclic form. These exhibited only moderate anti-SARS-CoV activity<sup>23</sup> while later work from the same laboratory showed  $N,N$ -dialkyl analogues **6b** and **6c** to have improved, albeit still low activity ( $K_i = 21.0 \mu\text{M}$ ,  $34.1 \mu\text{M}$ , respectively).<sup>32</sup>

$\alpha$ -Ketophthalhydrazide warheads with  $P_1$   $N,N$ -dimethyl-Gln isosteres, as illustrated by **7**, were investigated for anti-HAV



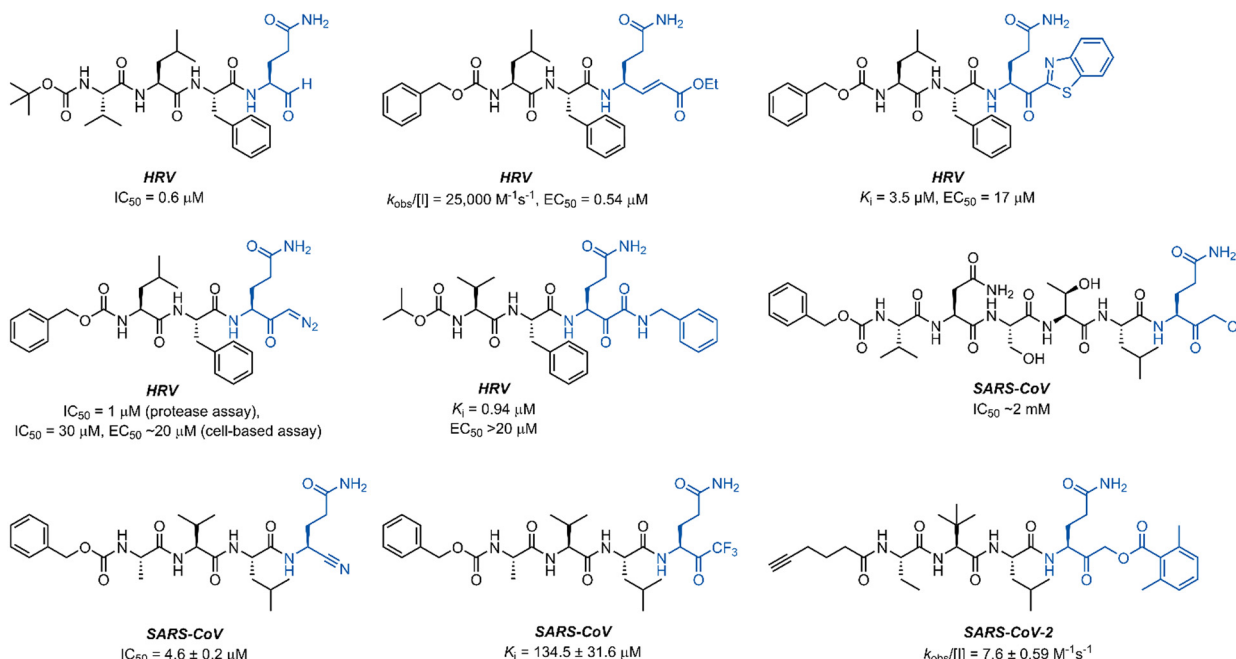
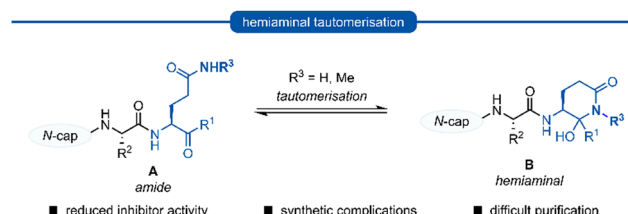
P<sub>1</sub> Gln inhibitors

Fig. 2 Representative 3C/3CL<sup>pro</sup> inhibitors possessing a P<sub>1</sub> (L)-glutamine residue with various electrophilic warheads.



Scheme 1 Generalised formation of hemiaminal B via tautomerisation of P<sub>1</sub> glutamine inhibitors A onto the electrophilic warhead.

3C<sup>pro</sup> activity.<sup>13,33</sup> Intermolecular hydrogen bonding of the ketone and proximal hydrazide NH was postulated to restrict conformational mobility, thereby decreasing the entropic penalty upon binding, while also mimicking the P<sub>2'</sub> phenylalanine (Phe) of the natural substrate.<sup>33</sup> Compound 7 was found to be a competitive reversible inhibitor against HAV ( $IC_{50} = 13 \mu M$ ), and no loss of activity was observed in the presence of a 100-fold excess of dithiothreitol (DTT), indicating its stability to extracellular thiols.

## Section 2. P<sub>1</sub> methionine derived inhibitors

Methionine (Met) and its oxidised sulfoxide and sulfone derivatives have also been investigated as non-nucleophilic glutamine P<sub>1</sub> isosteres due to their ease of synthesis and H-bonding ability (Fig. 4). Methionine sulfone analogue 8a was found to be a good reversible inhibitor of HRV 3C<sup>pro</sup> ( $K_i = 0.47 \mu M$ ) and also displayed good antiviral activity in tissue culture assays ( $IC_{50} = 3.4 \mu M$ ) with no observable cytotoxicity.<sup>34</sup> Additionally, inhibitor 8a was found to be more potent than inhibitors 8b and 8c

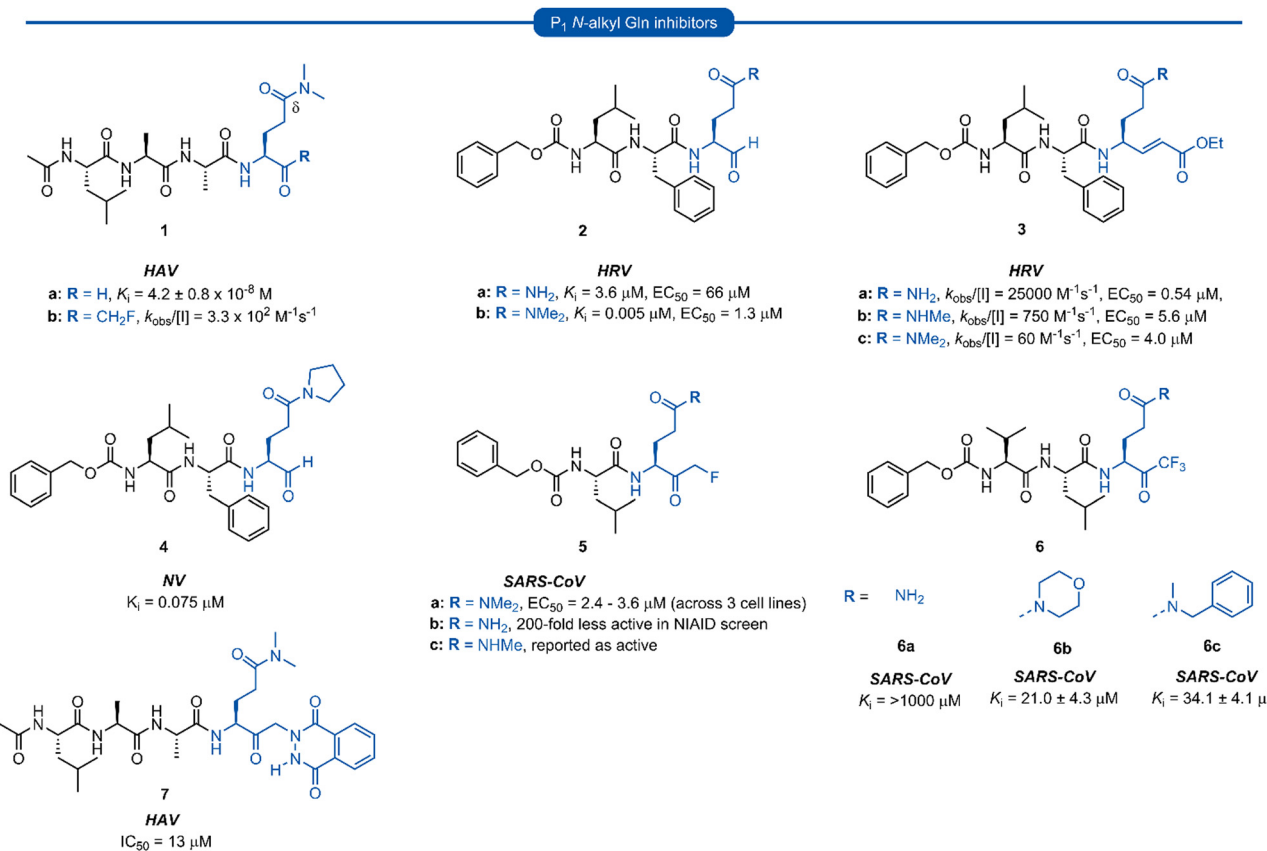
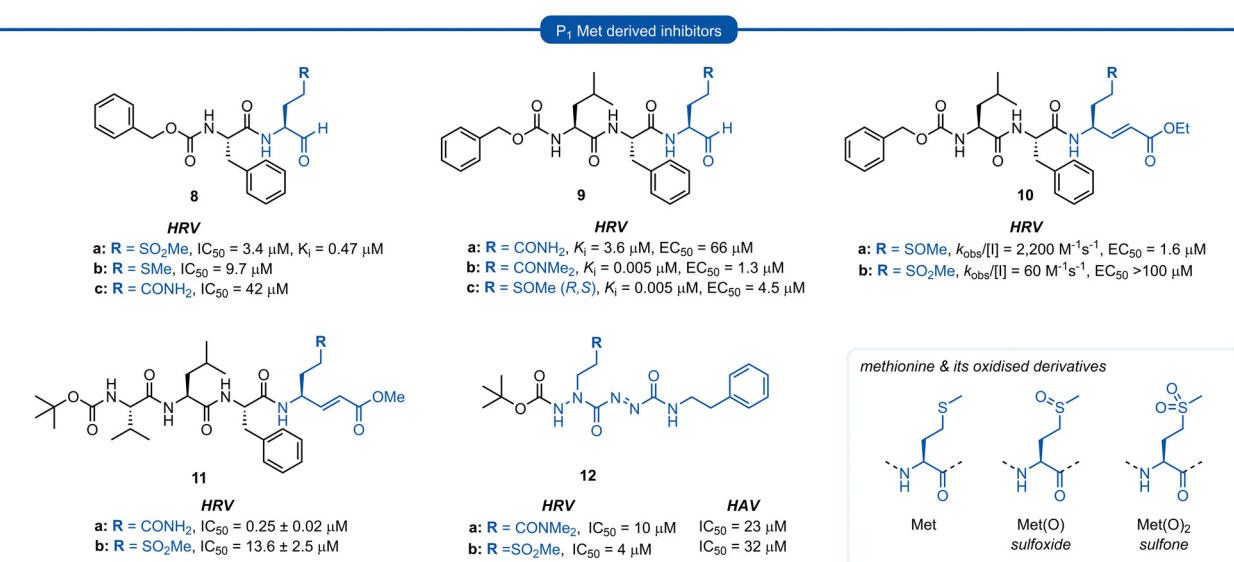
containing a P<sub>1</sub> methionine or glutamine residue, respectively ( $IC_{50} = 9.7 \mu M$  and  $IC_{50} = 42 \mu M$ ).

Similar observations were made in a separate study investigating aldehyde HRV 3C<sup>pro</sup> inhibitors. Sulfoxide 9c displayed superior potency compared to analogue 9a containing an unmodified Gln residue ( $IC_{50} = 0.005 \mu M$  vs.  $3.6 \mu M$ ), and was approximately equipotent to the N,N'-dimethyl-Gln analogue 9b. The potency of sulfoxide 9c was further supported by X-ray crystal structure data of the enzyme-inhibitor complex, which revealed the P<sub>1</sub> sulfoxide moiety fits snugly into the S<sub>1</sub> pocket and the H-bonding pattern of the active site His<sub>161</sub> and Thr<sub>142</sub> residues was analogous to that of the natural substrate.<sup>27</sup> The use of sulfoxide and sulfone P<sub>1</sub> isosteres in conjunction with Michael acceptor warheads on the other hand has met with less success. Two separate studies both reported that peptidyl inhibitors of HRV 3C<sup>pro</sup> containing a P<sub>1</sub> sulfoxide 10a or sulfone 10b and 11b residue showed a significant reduction in potency compared with their P<sub>1</sub> glutamine counterparts 3a and 11a, respectively.<sup>19</sup> Monopeptidyl aza-carboxamides, exemplified by 12a/b (For aza-backbone modifications, see Section 5) have also been investigated for anti HRV and HAV activity. P<sub>1</sub> sulfone 12b was found to have improved activity against HRV 3C<sup>pro</sup> compared to N,N'-dimethyl-Gln analogue 12a. Conversely, 12a was found to exhibit slightly higher potency against HAV 3C<sup>pro</sup> over 12b.<sup>35,36</sup>

## Section 3. P<sub>1</sub> inhibitors derived from non-proteogenic amino acids

A number of P<sub>1</sub> glutamine isosteres derived from unnatural amino acids were investigated during the early development of



Fig. 3 Representative examples of P<sub>1</sub> N-alkyl-Gln inhibitors targeting 3C/3CL<sup>pro</sup>.Fig. 4 Representative examples of P<sub>1</sub> Met derived inhibitors and their P<sub>1</sub> Gln/N-alkyl-Gln analogues targeting 3C/3CL<sup>pro</sup>.

3C/3CL<sup>pro</sup> inhibitors. Most notably, publications by Dragovich *et al.* and Webber *et al.* explored a diverse array of P<sub>1</sub> derivatives including glutamine related P<sub>1</sub> substrates (Section 1) and non-glutamine derived P<sub>1</sub> residues such as sulfones/sulfoxides

(Section 2), as well as a number of glutamine isosteres (representative examples, Fig. 5A). During these studies however, none of these analogues 13–15 or 16–18 showed increased potency over inhibitors containing the unmodified side chain

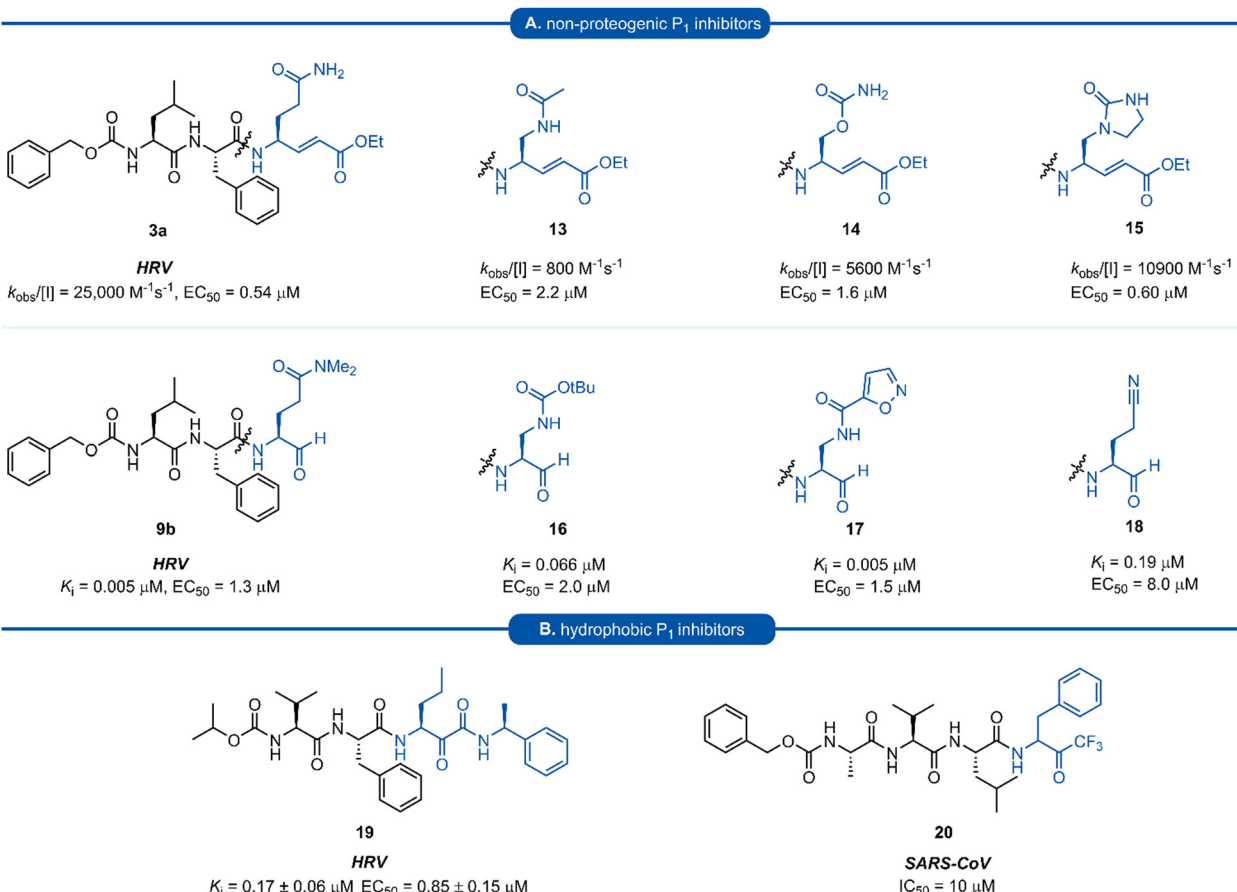


Fig. 5 (A) Inhibitors targeting 3C/3CL<sup>PRO</sup> containing non-proteogenic P<sub>1</sub> isosteres. (B) Hydrophobic P<sub>1</sub> residue inhibitors targeting 3C/3CL<sup>PRO</sup>.

3a<sup>19</sup> or the N,N'-dimethyl-Gln 9b<sup>27</sup> derivatives, respectively. Alternatively, peptidyl inhibitors bearing a hydrophobic amino acid in the P<sub>1</sub> position have also been investigated (Fig. 5B). The substitution of P<sub>1</sub> glutamine with non-nucleophilic residues circumvented synthetic complications caused by the reactivity of the electrophilic warhead. Representative examples 19 and 20 possess a norvaline (Nva) or phenylalanine hydrophobic amino acid at the P<sub>1</sub> position. Norvaline P<sub>1</sub> tetrapeptide inhibitor 19 was found to have low micromolar activity against HRV 3C<sup>PRO</sup> ( $K_i = 0.17$ ) and also having good activity in tissue culture ( $\text{EC}_{50} = 0.85 \mu\text{M}$ ),<sup>24</sup> while P<sub>1</sub>-phenylalanine inhibitor 20 was found to exhibit moderate time-dependent activity against SARS-CoV 3CL<sup>PRO</sup> ( $\text{IC}_{50} = 10 \mu\text{M}$ ).<sup>37</sup> A recent development in the inhibitor design has been made using self-masked aldehyde inhibitors (SMAIs) methodology for targeting 3CL protease.<sup>38</sup> Originally developed by Meek and co-workers to target cruzain, SMAIs was then applied to the development of SARS-CoV-2 inhibitor 21.<sup>39</sup> SMAIs methodology is designed to mask the reactive aldehyde warhead through the spontaneous formation of a  $\delta$ -lactol via nucleophilic attack by the P<sub>1</sub> 2-pyridone side-chain on the aldehyde warhead, which would closely mimic the  $\gamma$ -lactam P<sub>1</sub> moiety that is now commonly employed in the design of 3C/3CL protease inhibitors (see Section 7). Upon binding to the protease active site, acid catalysed ring-opening by an acidic residue, revealing the

reactive aldehyde warhead, which captures the cysteine residue to afford the enzyme-bound moiety (Scheme 2).

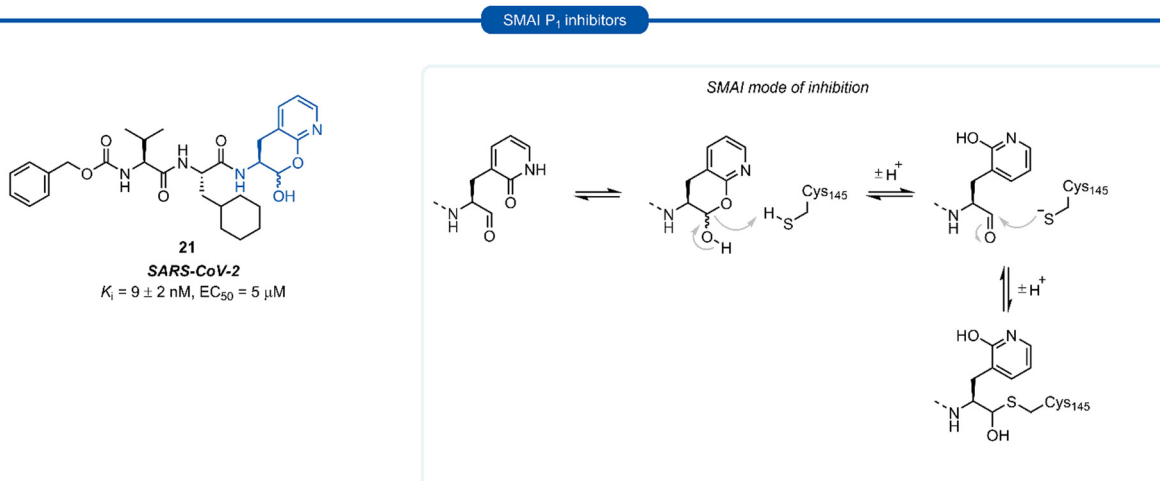
Formation of the lactol moiety was confirmed by NMR in organic solvents, however, unambiguous confirmation of the major species in aqueous solutions has not been made.<sup>38</sup> Compound 21 was found to be a competent inhibitor of SARS-CoV-2 with  $\text{EC}_{50}$  value of 5  $\mu\text{M}$ . A high-resolution X-ray crystal structure of 21 bound in the active site of SARS-CoV-2 3CL<sup>PRO</sup> confirmed the formation of the anticipated hemithioacetal between the aldehyde group and Cys<sub>145</sub>, thereby confirming the inhibitor's mechanism of action. The P<sub>1</sub> 2-pyridone residue also establishes the expected H-bonding pattern, with the 2-pyridone carbonyl group accepting H-bonding from His<sub>163</sub> and Ser<sub>144</sub> while the amide proton donates an H-bond to Glu<sub>166</sub> and Phe<sub>140</sub>.<sup>38</sup>

#### Section 4. P<sub>1</sub> histidine inhibitors

During work towards the development of SARS-CoV 3CL<sup>PRO</sup> inhibitors, investigations into the substrate preference for SARS-CoV 3CL<sup>PRO</sup> via positional scanning of synthetic recombinant libraries based on the 7-amino-4-carbamoyl-coumarin (ACC) fluorogenic leaving group were undertaken.

A surprising preference for histidine at P<sub>1</sub> was revealed which was further confirmed by synthesising single substrates and comparing their kinetic constraints (Fig. 6).<sup>40</sup> Early investigations





**Scheme 2** Putative mechanism of reversible covalent inhibition of a cysteine protease by SMAIs.

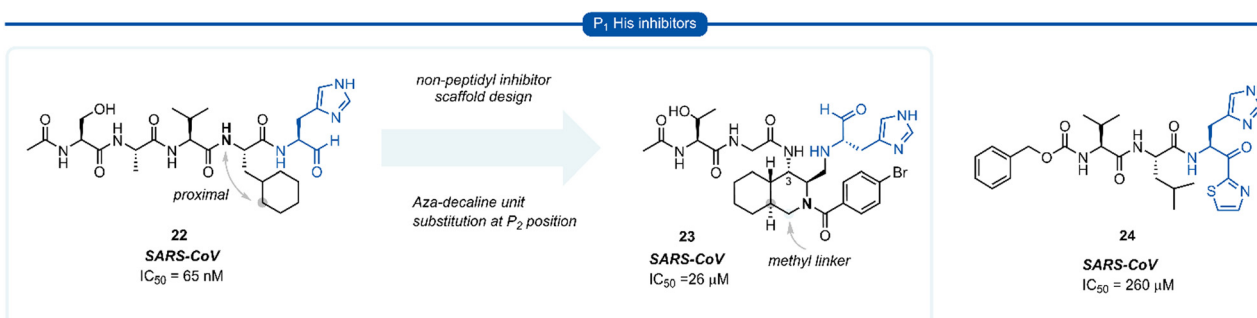


**Fig. 6** Representative examples of P<sub>1</sub> His inhibitors targeting SARS-CoV 3CL<sup>PRO</sup>.

of histidine P<sub>1</sub> analogues for anti SARS-CoV activity initially led to the discovery of the potent tetrapeptide inhibitor 22 ( $IC_{50} = 65 \text{ nM}$ ).<sup>41</sup> Analysis of the binding pocket of the inhibitor 22-bound X-ray crystal structure showed that the cyclohexyl ring of the P<sub>2</sub> cyclohexylalanine (Cha) was proximal to the  $\alpha$ -nitrogen of the corresponding amino acid residue. A novel dehydroisoquinoline inhibitor scaffold was designed by introduction of a methyl linker between the P<sub>2</sub> cyclohexyl ring and the P<sub>2</sub> backbone nitrogen and a peptide chain extending off the 3-position of the ring system of compound 23. Although compound 23 represents a novel class of 3CL<sup>PRO</sup> inhibitors, improved potency against SARS-CoV 3CL<sup>PRO</sup> compared with its linear predecessor 22, was not achieved.<sup>42–44</sup> Histidine P<sub>1</sub> residues were also employed by Hayashi *et al.* against 3CL<sup>PRO</sup> of SARS-CoV using  $\alpha$ -keto-thiazole warheads 24, however, these did not show superior activity to analogous P<sub>1</sub> lactam inhibitors (see Section 7) and were not further explored.<sup>45</sup>

## Section 5. P<sub>1</sub> aza-glutamine inhibitors

Azapeptides are peptide chains where one of the amino acid residues are replaced by a semicarbazide which conformationally restricts the peptide, bending the amino acid away from the natural linear geometry. Incorporation of semicarbazides into peptidyl inhibitor manifolds has been shown to improve

activity and selectivity while also showing improved pharmacokinetic properties such as metabolic stability and duration of action.<sup>46</sup> The success of aza-backbone modifications at the P<sub>1</sub> position of papain inhibitors initially led to their incorporation in the design of inhibitors for the closely related 3C/3CL<sup>PRO</sup> (Fig. 7).<sup>47,48</sup> Norbeck *et al.* developed P<sub>1</sub> aza-glutamine bromomethylketone 25 for anti-HRV activity as a time-dependent irreversible inhibitor ( $k_{inact}/K_{inact} = 23\,400 \text{ M}^{-1} \text{ s}^{-1}$ ).<sup>49,50</sup> In a separate study, a series of aza-glutamine inhibitors such as 26 were found to have moderate activity against both HRV and HAV 3C<sup>PRO</sup> ( $IC_{50} = 12 \mu\text{M}$  and  $IC_{50} = 10 \mu\text{M}$ ) respectively.<sup>35</sup> Although a number of P<sub>1</sub> aza-glutamine inhibitors have been investigated, generally only moderate potency has been achieved against HRV and HAV.<sup>48,51</sup> P<sub>1</sub> aza-glutamine inhibitors have also been developed against SARS-CoV. Notably, James *et al.* demonstrated through X-ray crystal structure elucidation that aza-glutamine epoxide 27 irreversibly binds *via* an induced-fit model.<sup>52,53</sup> Müller and co-workers have also developed a potent inhibitor of 3CL<sup>PRO</sup> SARS CoV-2 containing a N-methyl-azanitrile warhead unit 28 ( $K_i = 24 \text{ nM}$ ).<sup>54</sup>

## Section 6. P<sub>1</sub> Gln macrocyclic inhibitors

Macrocyclic inhibitors have been shown to display improved properties over their acyclic counterparts for the inhibition of



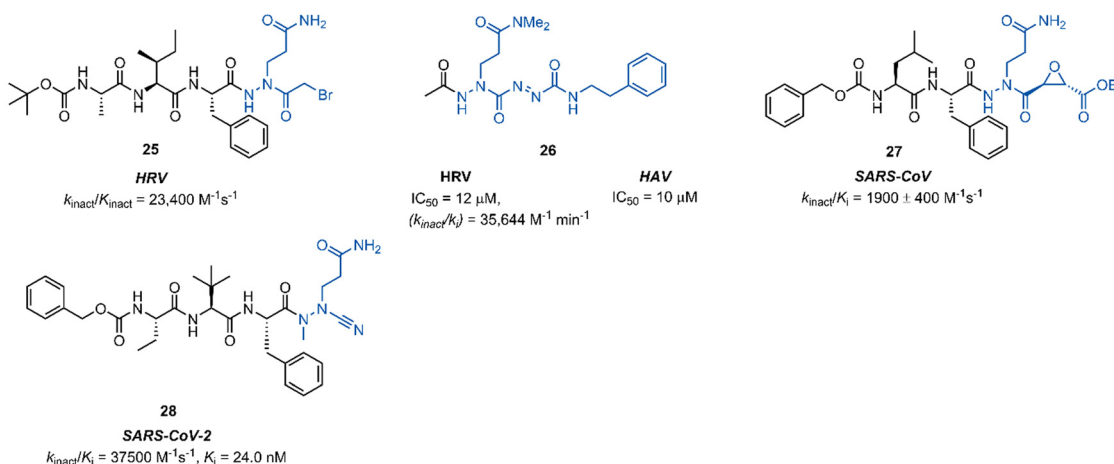


Fig. 7 Representative examples of P<sub>1</sub> aza-Gln inhibitors targeting 3C/3CL<sup>pro</sup>.

protease enzymes. Protease enzymes recognise their ligands in a  $\beta$ -strand conformation, and macrocyclization can help facilitate the backbone hydrogen bonding pattern of peptide inhibitors to mimic that of an extended antiparallel  $\beta$ -sheet of the natural substrate.<sup>55-57</sup> Macrocyclization may also increase the structural rigidity of peptide-based inhibitors, restricting the conformational interchange and thereby enhancing the affinity for the receptor by reducing the loss of entropy upon binding, as well as exhibiting improved receptor selectivity and favourable drug-like characteristics including increased cell permeability and proteolytic stability.<sup>55,58-60</sup> The first investigations

into macrocyclic 3C<sup>pro</sup> and 3CL<sup>pro</sup> inhibitors arose from analysis of the crystal structure of inhibitors bound to HRV 3C<sup>pro</sup>, revealing close spatial proximity between P<sub>1</sub> and P<sub>3</sub> side-chains. Modelling studies yielded tripeptidyl macrocyclic inhibitor 29, where a triazole-containing linker adjoined the P<sub>1</sub> and P<sub>3</sub> residues (Fig. 8). The inhibitor activity was evaluated against norovirus, enterovirus and SARS-CoV, and in all cases 29 was found to inhibit the protease in the low micromolar range.<sup>61</sup> Further investigation showed poor correlation between 3CL<sup>pro</sup> enzyme inhibition assays (IC<sub>50</sub>) and inhibition of norovirus replication in a cell-based replicon system assays (EC<sub>50</sub>) for 29.

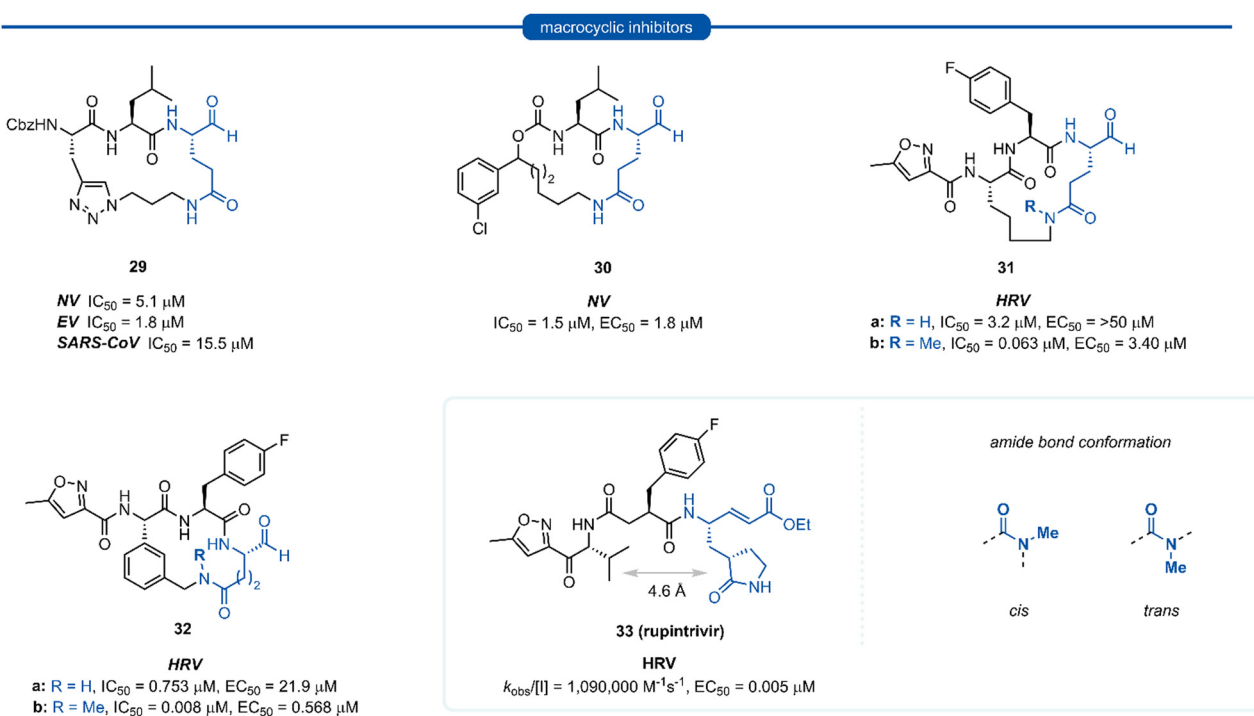


Fig. 8 Representative examples of macrocyclic lactam inhibitors containing a P<sub>1</sub> Gln residue

and derivatives thereof.<sup>62</sup> This result indicates that compounds such as **29** likely suffer from poor cellular permeability due to the triazole ring increasing the polar surface area. An X-ray crystal structure of NV 3CL<sup>Pro</sup> with bound inhibitor **29** revealed the expected antiparallel  $\beta$ -sheet backbone binding conformation, and the tetrahedral adduct between the aldehyde warhead and Cys<sub>139</sub> residue was also present. It was noted however, that binding induced suboptimal structural changes of the protease binding pocket and more importantly, the S<sub>1</sub> pocket, resulting in loss of the key Thr<sub>134</sub> and His<sub>157</sub> H-bonds to P<sub>1</sub> Gln and thus maximal binding efficiency was not obtained.<sup>62,63</sup> Further publications explored related macrocyclic inhibitors with alkyl linkers which generally gave increased cell permeability, with inhibitor **30** found to have good activity in both enzyme and cell-based assays. Co-crystallisation of **30** and NV 3C<sup>Pro</sup> showed the expected backbone H-bonding pattern indicating the expected bonding orientation. The key H-bonding interaction between the P<sub>1</sub> amide of **30** and His<sub>157</sub> and Thr<sub>134</sub> of NV 3C<sup>Pro</sup> however was again absent; instead, a new H-bond between the oxygen of the tetrahedral thioacetal adduct and Pro<sub>136</sub> was evident.<sup>64</sup> Rupintrivir **33** (AG-7088), a potent anti-rhinoviral agent that became the subject of extensive preclinical and clinical investigation, was used as a scaffold for macrocyclic inhibitors, with the goal of improving rupintrivir's pharmacokinetic properties.<sup>65</sup> The crystal structure of rupintrivir/HRV2 3C<sup>Pro</sup> showed only 4.6 Å between the P<sub>1</sub> and P<sub>3</sub> side chains, providing an opportunity for the introduction of a macrocyclic linkage.

The resulting macrocycle **31a** was tested against HRV 3C<sup>Pro</sup> and showed decreased potency compared to rupintrivir (EC<sub>50</sub> > 50  $\mu$ M) in HeLa cells infection model, albeit conserving moderate protease inhibition activity with IC<sub>50</sub> values in the low micromolar range (IC<sub>50</sub> = 3.2  $\mu$ M). Modelling of the macrocyclic peptide in the binding pocket predicted the glutamine-derived amide bond was required to be in the *cis* conformation for efficient binding. Despite the *cis* conformation being higher energy, methylation of the amide nitrogen allows increased population of the *cis* conformer. Inhibitor **31b** containing an N-methyl moiety showed a 50-fold increase in potency against HRV 3C<sup>Pro</sup> (IC<sub>50</sub> = 0.063  $\mu$ M) despite losing an H-bonding interaction between the P<sub>1</sub> amide proton and backbone carbonyl of Thr<sub>142</sub>. Alternatively, incorporation of a phenyl ring into the macrocyclic linkage gave inhibitor **32a** (IC<sub>50</sub> = 0.753  $\mu$ M), which displayed a 4-fold increase in activity over **31a**. Additional incorporation of the N-methyl moiety afforded **32b** and further increased the activity by 100-fold (IC<sub>50</sub> = 0.008  $\mu$ M).

## Section 7. P<sub>1</sub> lactam inhibitors

Pioneering work by Dragovich and co-workers first led to the use of  $\gamma$ -lactams as P<sub>1</sub> glutamine isosteres in a series of publications developing tripeptide inhibitors of HRV 3C<sup>Pro</sup>.<sup>18,19,66,67</sup> Early investigations (see Sections 3 and 4) found that none of the P<sub>1</sub> non-glutamine inhibitors showed improved potency over the inhibitor containing an unmodified glutamine side chain **3a** (Fig. 9A). Inspection of the X-ray crystal structure of **3a** bound to HRV 3C<sup>Pro</sup> revealed that while the P<sub>1</sub> *trans* amide

proton is engaged in a H-bond to the backbone carbonyl of Thr<sub>142</sub>, the *cis* amide proton is solvent exposed, providing a vector for further optimisation of the P<sub>1</sub> side chain. N-Monomethyl inhibitor **3b** displayed significantly weaker protease inhibition, presumably due to the amide preferentially adopting a *trans* conformation, interrupting the key P<sub>1</sub> amide proton-Thr<sub>142</sub> H-bond (Fig. 9A). In order to lock in the desired *cis* amide conformation, an (S)- $\gamma$ -lactam was incorporated into the P<sub>1</sub> side chain.

The resulting tripeptide **34a** displayed a remarkable increase in protease inhibition activity against HRV 3C<sup>Pro</sup> as well as sub-micromolar antiviral activity in cell culture.<sup>67</sup> The combination of this newly optimised P<sub>1</sub> side chain with favourable P<sub>2</sub>-P<sub>4</sub> modifications discovered in related work gave rise to rupintrivir **33** (AG-7088). During the initial investigation into P<sub>1</sub> lactam-based glutamine isosteres, it was found that while a (S)- $\delta$ -lactam moiety **34b** was equally effective as the (S)- $\gamma$ -lactam **34a**, switching the stereochemistry of the lactam ring **34c** or replacing the lactam moiety with a 5-membered cyclic urea **34d** resulted in a significant reduction in activity (Fig. 9B).<sup>67</sup> Following the work of Dragovich *et al.* and guided by crystal structure studies revealing the high degree of structural homology among 3C<sup>Pro</sup> and 3CL<sup>Pro</sup> enzymes, P<sub>1</sub> (S)-lactam isosteres have been integrated into the design of numerous inhibitors targeting 3C/3CL<sup>Pro</sup>. The first example outside of the preliminary work on HRV protease was for the development of inhibitors of hepatitis A virus (HAV) 3C<sup>Pro</sup>. From a small series of compounds bearing an  $\alpha$ -ketophthalahydrazide, compound **35** proved to be the most effective (IC<sub>50</sub> = 1.6  $\mu$ M).<sup>68</sup> Representative examples of 3C/3CL<sup>Pro</sup> inhibitors bearing a P<sub>1</sub> (S)-lactam isostere are shown in Fig. 10, showcasing the compatibility of the P<sub>1</sub> (S)-lactam with a range of electrophilic warhead functionalities. The (S)-lactam P<sub>1</sub> unit has been shown to be effective in targeting numerous viral 3C/3CL<sup>Pro</sup> including compounds **36–38** for enterovirus,<sup>69–74</sup> **39** for norovirus,<sup>75–79</sup> **40–41** for SARS-CoV,<sup>32,45,80–89</sup> **42** for MERS-CoV,<sup>90–92</sup> and **43–51** for SARS-CoV-2 (Fig. 11). A handful of inhibitors demonstrating broad spectrum activity have also been developed.<sup>93–96</sup> As represented in Fig. 10, 3C/3CL<sup>Pro</sup> inhibitors typically employ a (S)- $\gamma$ -lactam P<sub>1</sub> isostere, however enterovirus has been shown to prefer the (S)- $\delta$ -lactam isostere at the P<sub>1</sub> position. This was first demonstrated through docking studies of EV71 3C<sup>Pro</sup>, revealing the  $\delta$ -lactam had shorter H-bond distances with His<sub>161</sub> and Thr<sub>142</sub> compared to the  $\gamma$ -lactam, while also adopting a preferable binding orientation in the S<sub>1</sub> pocket.<sup>70,71</sup> This model was validated through the design of inhibitor **36c**, which was 7–10 fold more active than the corresponding  $\gamma$ -lactam **36b**. In a separate study, screening of a compound library revealed compound **37** containing a chiral cyanohydrin warhead.<sup>72</sup> Each epimer was tested separately and exhibited good activity against EV71 with little effect of the warhead stereochemistry on the potency of the inhibitor. The same library screening also revealed an inhibitor scaffold analogous to that of **37** with an aldehyde warhead **38**, to be the most potent compound tested against EV71 in both 3C<sup>Pro</sup> protease inhibition assay and human rhabdomyosarcoma cells viral infection model.<sup>70–72</sup>



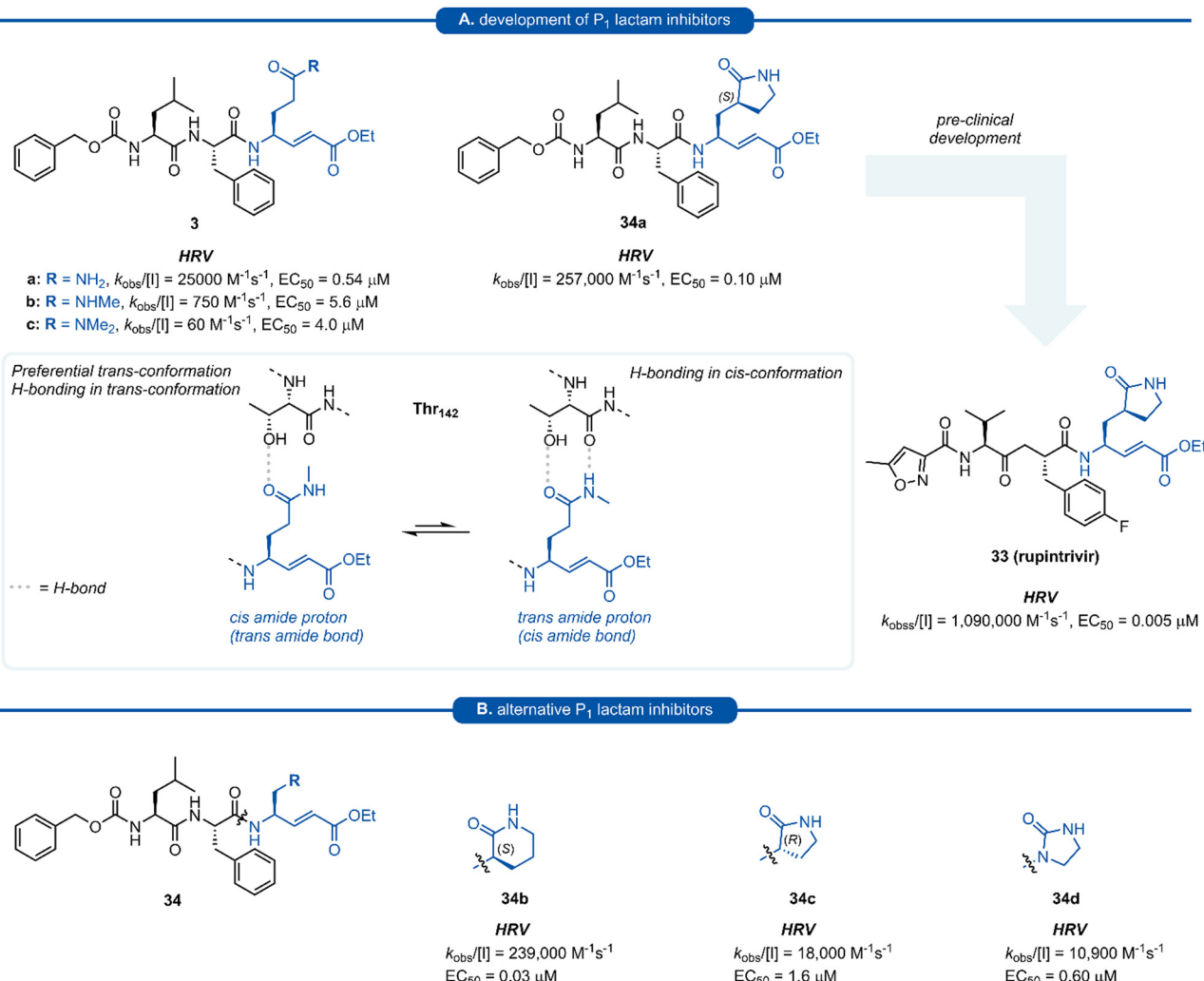


Fig. 9 (A) Development of HRV inhibitors possessing a  $P_1$  (*S*)- $\gamma$ -lactam moiety. (B) Alternative  $P_1$  lactam isosteres.

Since the SARS-CoV-2 outbreak in 2019, new inhibitors of the main protease  $3\text{CL}^{\text{pro}}$  (aka  $\text{M}^{\text{pro}}$ ,  $\text{Nsp5}$ ) have almost exclusively been developed using  $P_1$  (*S*)- $\gamma$ -lactam isostere. In early work, it was realised that a high degree of homology existed between  $3\text{CL}^{\text{pro}}$  of SARS-CoV and SARS-CoV-2.<sup>97</sup> In addition to their 96% sequence identity, X-ray crystal data has demonstrated there to be a high structural similarity between SARS-CoV and SARS-CoV-2  $3\text{CL}^{\text{pro}}$  with a root mean square deviation of 0.53 Å across all  $\text{C}\alpha$  positions.<sup>98</sup> This suggested that structural features from known coronaviral protease inhibitors are likely to be effective when incorporated into the design of SARS-CoV-2  $3\text{CL}^{\text{pro}}$  inhibitors. This was demonstrated in an early report by Hilgenfeld and co-workers in the development of  $\alpha$ -ketoamide inhibitor **43** from known inhibitor **42**. The (*S*)- $\gamma$ -lactam moiety was found to occupy the  $3\text{CL}^{\text{pro}}$   $S_1$  pocket, with the crystal structure of SARS-CoV-2  $3\text{CL}^{\text{pro}}$  with **43** highlighting the crucial H-bonding between the lactam carbonyl oxygen with  $\text{His}_{163}$  side-chain imidazole, and the lactam nitrogen forming a three-centred hydrogen bond with  $\text{Phe}_{140}$  and  $\text{Glu}_{166}$ .<sup>98</sup> Various electrophilic warhead moieties have been demonstrated as

effective in combination with a  $P_1$  (*S*)- $\gamma$ -lactam group targeting SARS-CoV-2  $3\text{CL}^{\text{pro}}$ . Dipeptides bearing a heterocyclic acyloxymethylketone warhead were shown to be excellent irreversible inhibitors of SARS-CoV-2  $3\text{CL}^{\text{pro}}$ , exemplified by **44**.<sup>99</sup> Compound **44** also exhibited excellent plasma stability, glutathione stability, and selectivity over human proteases cathepsin B and cathepsin S. Inhibitor **45**, which possesses a Michael acceptor warhead unit and inhibits SARS-CoV-2  $3\text{CL}^{\text{pro}}$  in the low micromolar range ( $\text{IC}_{50} = 0.9 \mu\text{M}$ ), was recently demonstrated to exhibit significantly superior antiviral activity in hACE2 cell assays ( $\text{EC}_{50} = 8.2 \text{ nM}$ ).<sup>100</sup> Upon further investigation, this enhanced potency was attributed to a dual mode of action of compound **45** in targeting the SARS-CoV-2 virus lifecycle. In addition to inhibiting  $3\text{CL}^{\text{pro}}$ , **45** was found to also inhibit cathepsin L (CatL), a protease enzyme responsible for cleaving the viral Spike protein, promoting cell entry. Intraperitoneal administration of **45** in SARS-CoV-2 infected transgenic mice also showed to cause reduced viral load in the lungs and enhanced survival rate. In line with the development of inhibitors of other viral proteases, the introduction of an



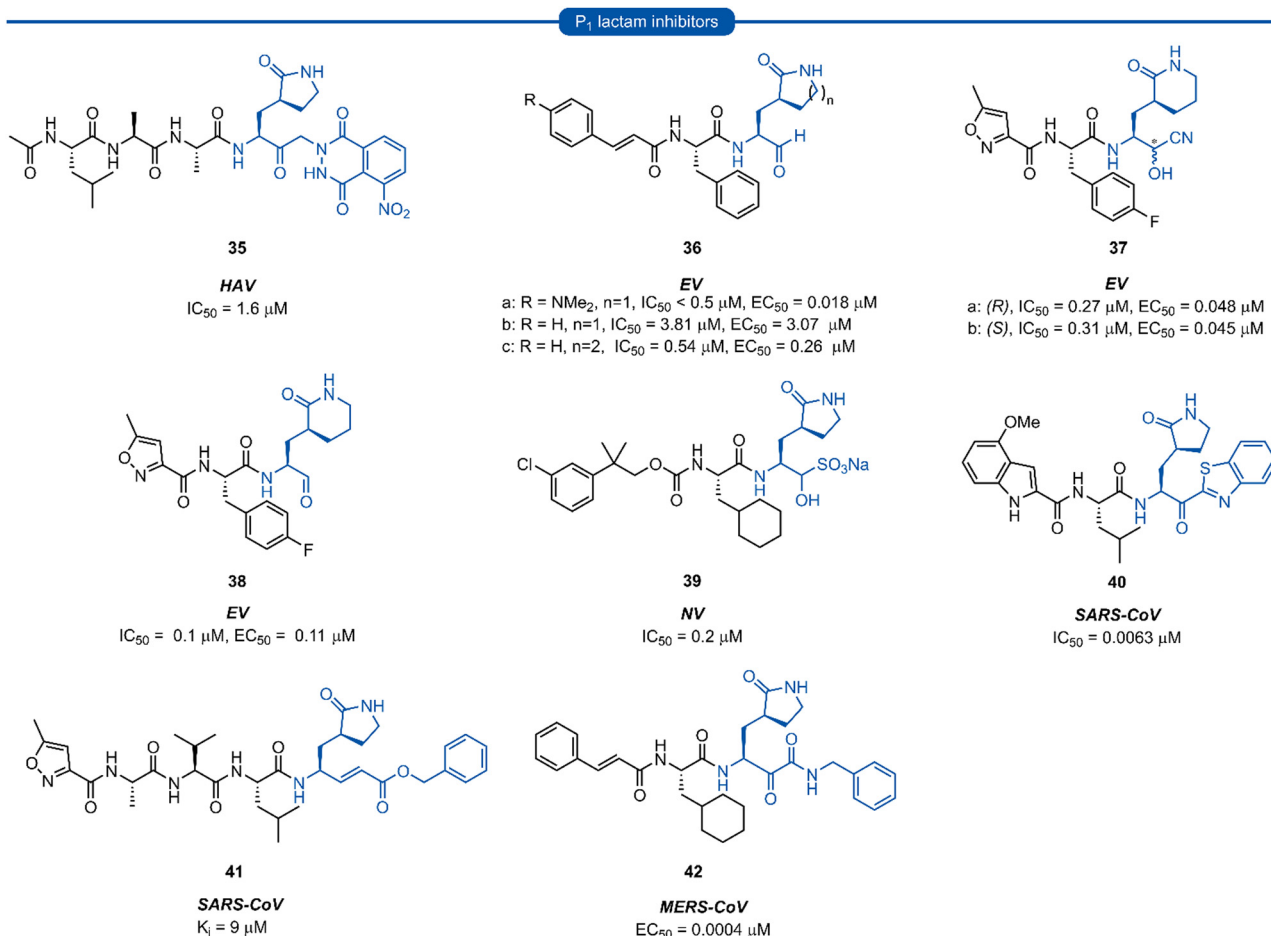


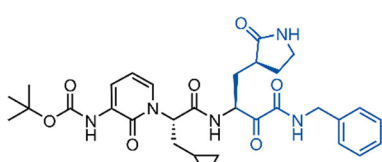
Fig. 10 Representative examples of inhibitors targeting 3C/3CL<sup>pro</sup> containing a P<sub>1</sub> (S)- $\gamma$ / $\delta$ -lactam isostere.

aldehyde C-terminal warhead has also proved effective for the discovery of SARS-CoV-2 3CL<sup>pro</sup> inhibitors (46–48). Structure-based design utilising the crystal structure of SARS-CoV 3CL<sup>pro</sup> gave rise to dipeptide aldehyde 46, which demonstrates good anti-SARS-CoV-2 activity ( $EC_{50} = 0.53$  nM) and was selected for further preclinical development.<sup>101</sup> Compounds 47 (*aka* MI-30)<sup>102</sup> and 48 (*aka* UAWJ9-36-3)<sup>103</sup> represent a series of aldehyde-based hybrid inhibitors which combine the P<sub>1</sub> (S)- $\gamma$ -lactam group with a bicyclic proline P<sub>2</sub> residue derived from the hepatitis C virus (HCV) inhibitors, telaprevir<sup>104</sup> (P<sub>2</sub> 5,5-fused ring) or boceprevir<sup>105</sup> (P<sub>2</sub> 3,5-fused ring), respectively. Unlike work towards other viral 3C/3CL<sup>pro</sup> inhibitors highlighted in this review, SARS-CoV-2 inhibitors are now at various stages of clinical development (Fig. 11). Compound 49 (*aka* PF-00835231), containing a P<sub>1</sub> (S)- $\gamma$ -lactam group in conjunction with a hydroxymethylketone C-terminal electrophilic warhead, was identified as a potent inhibitor of SARS-CoV-2 3CL<sup>pro</sup> ( $IC_{50} = 4$  nM) and was selected as the basis for the development of a protease inhibitor for the treatment of COVID-19.<sup>106</sup> One drawback of compound 49 that became apparent during preclinical characterisation was its relatively poor intrinsic aqueous solubility ( $< 0.1$  mg mL<sup>-1</sup>), which was insufficient to formulate for intravenous (IV) infusion. Accordingly, IV administration was

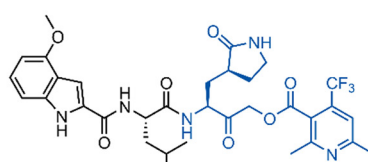
enabled by utilizing a prodrug strategy, resulting in the phosphate prodrug lufotrelvir (compound 50) which displays vastly superior aqueous solubility of  $> 200$  mg mL<sup>-1</sup> over a pH range suitable for IV infusion.<sup>107</sup> Lufotrelvir (50) is rapidly converted to the active free hydroxymethyl ketone (PF-00835231, 44) following administration. Work towards development of an orally bioavailable SARS-CoV-2 inhibitor has been undertaken by Owen and co-workers (Pfizer). Again using 49 as a lead compound, several modifications were made in order to reduce the hydrogen bond donor (HBD) count which has been shown to correlate with poor oral bioavailability.<sup>108</sup> Changing the electrophilic warhead from a hydroxymethyl ketone (HMK) to a nitrile group significantly increased its oral bioavailability (Oral F = 1.4% *vs.* 7.6% for otherwise identical HMK and nitrile inhibitors, respectively). It was also noted that compounds containing a nitrile warhead were less likely to undergo epimerization at the P<sub>1</sub> group during chemical synthesis compared to those equipped with heterocyclic ketone warheads that were also being investigated.<sup>108</sup> Incorporation of a P<sub>2</sub> bicyclic proline derivative and N-terminal cap modifications afforded nirmatrelvir (51), which displays superior activity ( $EC_{50} = 74.5$  nM) and oral bioavailability (F = 50%) over its predecessor 49 ( $EC_{50} = 231$  nM, oral F = 1.4%).<sup>109</sup>



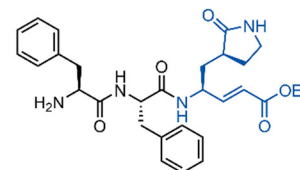
## A. SARS-CoV-2 preclinical development



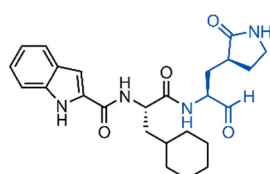
**43**  
SARS-CoV-2  
 $IC_{50} = 670$  nM,  $EC_{50} = 1.8$   $\mu$ M



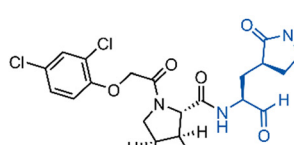
**44**  
SARS-CoV-2  
 $IC_{50} = 0.017$   $\mu$ M,  $EC_{50} = 0.28$   $\mu$ M



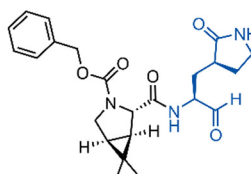
**45**  
SARS-CoV-2  
 $IC_{50} = 0.9$   $\mu$ M,  $EC_{50} = 8.2$  nM



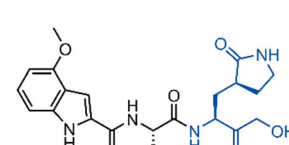
**46**  
SARS-CoV-2  
 $IC_{50} = 53$  nM



**47 (MI-30)**  
SARS-CoV-2  
 $IC_{50} = 17$  nM,  $EC_{50} = 0.54$   $\mu$ M



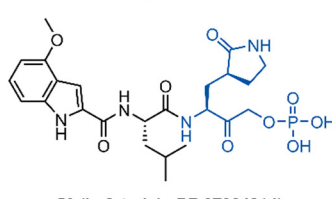
**48**  
SARS-CoV-2  
 $IC_{50} = 54$  nM,  $EC_{50} = 0.37$   $\mu$ M



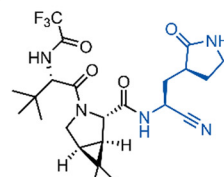
**49 (PF-00835231)**  
SARS-CoV-2  
 $EC_{50} = 231$  nM

## B. SARS-CoV-2 clinical development

Compound 49



**50 (Lufotrelvir, PF-07304814)**  
SARS-CoV-2  
 $K_i = 174$  nM,  $EC_{50} = 86.7$  nM

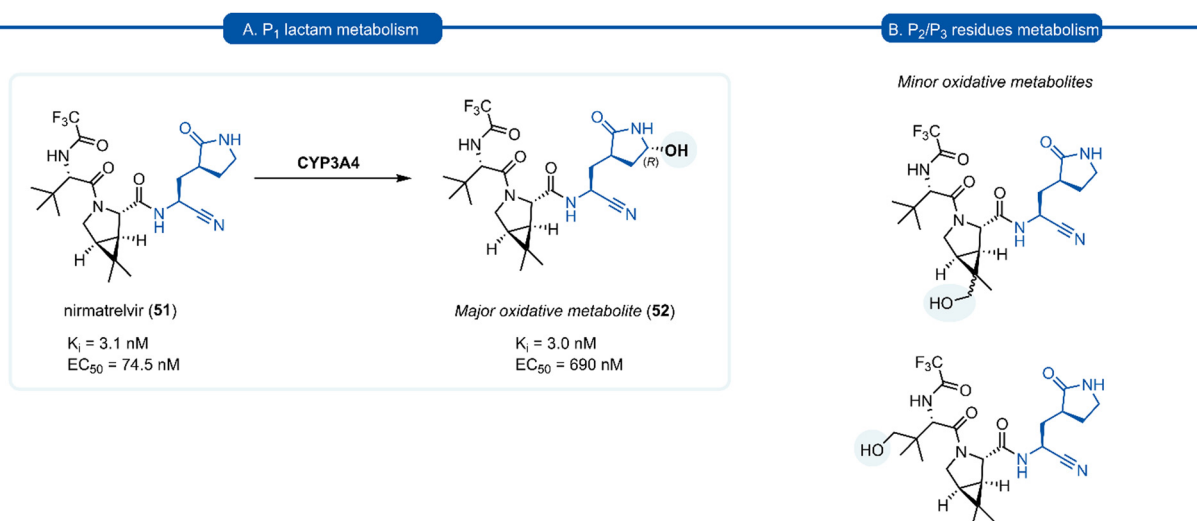


**51 (Nirmatrelvir, PF-07321332)**  
SARS-CoV-2  
 $EC_{50} = 74.5$  nM

Fig. 11 Representative examples of SARS-CoV-2 inhibitors in preclinical (A) or clinical (B) development.

A drawback of the  $P_1$  (*S*)- $\gamma$ -lactam glutamine isostere which became apparent through preclinical development of nirmatrelvir (**51**), is its susceptibility to undergo cytochrome P450

(CYP450) oxidative metabolism. The primary route of inactivation of nirmatrelvir in human liver microsomes occurs *via* CYP3A4-mediated oxidation. The major metabolite **52** resulting



Scheme 3 (A) The primary route of metabolism of nirmatrelvir **51** *via* CYP3A4 hydroxylation of the  $P_1$  (*S*)- $\gamma$ -lactam moiety. (B) Minor metabolites products of nirmatrelvir **51** *via* CYP3A4 hydroxylation of the  $P_2$  and  $P_3$  moiety.

from hydroxylation of the pyrrolidine ring and which, albeit exhibiting similar inhibition potency against 3CL<sup>pro</sup> and representing viral replication, was 10-fold less active against SARS-CoV-2 compared to **51** in epithelial Vero E6 cells infection model (Scheme 3). In the same study, other minor metabolites of nirmatrelvir, produced by CYP3A4 *via* alternative oxidation patterns at the P<sub>1</sub> and P<sub>2</sub> position, were detected in trace amounts, but their individual inhibitory potencies were not measured due to their low relative abundance.<sup>109</sup> This has ultimately led to nirmatrelvir being co-administered with the CYP3A4 inhibitor, ritonavir, to increase its bioavailability. This combined formulation, Paxlovid™ has proven to be a safe and effective treatment for COVID-19 for patients with high risk of disease progression, resulting in an 89% risk reduction in treated patients relative to a placebo group.<sup>110</sup>

## Conclusion

Over the last 25 years, considerable effort has been invested into the development of P<sub>1</sub> glutamine isosteres for incorporation into inhibitors targeting 3C<sup>pro</sup> and 3CL<sup>pro</sup> of viruses in the *Pisoniviricetes* class. Early efforts exploring P<sub>1</sub> N-alkyl glutamine inhibitors were met with mixed success, while more structurally diverse methionine and carbonyl derived isosteres of glutamine, were generally found to be detrimental to inhibitor activity. Macrocyclization and aza group backbone modifications at the P<sub>1</sub> position, although delivering low micromolar inhibitors, also did not demonstrate any significant improvements over their linear and unmodified counterparts. Incorporation of the P<sub>1</sub> lactam isostere resulted in significantly more potent inhibitors and the development of the (S)- $\gamma$ -lactam moiety marked the first real progress towards potent 3C/3CL<sup>pro</sup> inhibitors. The lactam was found to conformationally restrict the P<sub>1</sub> side chain amide bond in the *cis* conformation, providing optimal H-bonding interactions in the S<sub>1</sub> binding pocket and reducing the entropic cost of binding. Moreover, the inhibitor inactivation by intramolecular cyclisation of the nucleophilic P<sub>1</sub> amide moiety onto the electrophilic warhead, was not observed for the (S)-lactam. The P<sub>1</sub> (S)-lactam moiety has now found widespread use in targeting 3C/3CL<sup>pro</sup> due to its optimal binding interactions and broad compatibility with electrophilic warheads. Recent metabolic studies on nirmatrelvir, however, have now revealed the lactam group to be the primary metabolic hotspot. Although the P<sub>1</sub> lactam moiety has provided one of the major milestones in targeting 3C<sup>pro</sup> and 3CL<sup>pro</sup>, further structural optimisation of the lactam side chain is desirable to improve the pharmacokinetics of P<sub>1</sub> lactam containing inhibitors.

## Author contributions

L. A. Stubbing: concept and original version. J. Bell-Tyler: writing – original draft. Y. O. Hermant, J. G. Hubert, S. H. Yang, A. M. McSweeney, G. M. McKenzie-Goldsmith, D. P. Furkert, V. K. Ward, M. A. Brimble: writing – review and editing.

V. K. Ward, M. A. Brimble: project administration, funding acquisition.

## Conflicts of interest

There are no conflicts to declare.

## Acknowledgements

The authors thank the Ministry of Business, Innovation and Employment (MBIE), contract number U00X1904 and Auckland Medical Research Foundation, grant 1720013 for financial support.

## References

- 1 World Health Organization, The top 10 causes of death, <https://www.who.int/news-room/fact-sheets/detail/the-top-10-causes-of-death>, 2020, accessed 13/03/2023.
- 2 T. Heikkinen and A. Jarvinen, *Lancet*, 2003, **361**, 51.
- 3 X. Wang, J. Ren, Q. Gao, Z. Hu, Y. Sun, X. Li, D. J. Rowlands, W. Yin, J. Wang, D. I. Stuart, Z. Rao and E. E. Fry, *Nature*, 2015, **517**, 85.
- 4 A. Bouin and B. L. Semler, *Curr. Clin. Microbiol. Rep.*, 2020, **7**, 31.
- 5 T. M. Szopa, P. A. Titchener, N. D. Portwood and K. W. Taylor, *Diabetologia*, 1993, **36**, 687.
- 6 J. D. Kriesel, A. White, F. G. Hayden, S. L. Spruance and J. Petajan, *Mult. Scler.*, 2004, **10**, 145.
- 7 S. Payne, *Viruses*, 2017, 149.
- 8 S. M. Ahmed, A. J. Hall, A. E. Robinson, L. Verhoef, P. Premkumar, U. D. Parashar, M. Koopmans and B. A. Lopman, *Lancet Infect. Dis.*, 2014, **14**, 725.
- 9 S. C. Baker, *Encyclopedia of Virology*, Oxford Academic Press, Oxford, Third edn, 2008, p. 554.
- 10 D. Sun, S. Chen, A. Cheng and M. Wang, *Viruses*, 2016, **8**, 82.
- 11 C. P. Campillay-Veliz, J. J. Carvajal, A. M. Avellaneda, D. Escobar, C. Covian, A. M. Kalergis and M. K. Lay, *Front. Immunol.*, 2020, **11**, 961.
- 12 D. A. Matthews, W. W. Smith, R. A. Ferre, B. Condon, G. Budahazi, W. Sisson, J. E. Villafranca, C. A. Janson, H. E. McElroy and C. L. Gribskov, *et al.*, *Cell*, 1994, **77**, 761.
- 13 J. Yin, M. M. Cherney, E. M. Bergmann, J. Zhang, C. Huitema, H. Pettersson, L. D. Eltis, J. C. Vederas and M. N. James, *J. Mol. Biol.*, 2006, **361**, 673.
- 14 K. Anand, J. Ziebuhr, P. Wadhwani, J. R. Mesters and R. Hilgenfeld, *Science*, 2003, **300**, 1763.
- 15 X. Fan, X. Li, Y. Zhou, M. Mei, P. Liu, J. Zhao, W. Peng, Z. B. Jiang, S. Yang, B. L. Iverson, G. Zhang and L. Yi, *ACS Chem. Biol.*, 2020, **15**, 63.
- 16 H. Chen, Z. Zhu, Y. Qiu, X. Ge, H. Zheng and Y. Peng, *Virol. Sin.*, 2022, **37**, 437.

17 S. W. Kaldor, M. Hammond, B. A. Dressman, J. M. Labus, F. W. Chadwell, A. D. Kline and B. A. Heinz, *Bioorg. Med. Chem. Lett.*, 1995, **5**, 2021.

18 P. S. Dragovich, S. E. Webber, R. E. Babine, S. A. Fuhrman, A. K. Patick, D. A. Matthews, C. A. Lee, S. H. Reich, T. J. Prins, J. T. Marakovits, E. S. Littlefield, R. Zhou, J. Tikhe, C. E. Ford, M. B. Wallace, J. W. Meador, 3rd, R. A. Ferre, E. L. Brown, S. L. Binford, J. E. Harr, D. M. DeLisle and S. T. Worland, *J. Med. Chem.*, 1998, **41**, 2806.

19 P. S. Dragovich, S. E. Webber, R. E. Babine, S. A. Fuhrman, A. K. Patick, D. A. Matthews, S. H. Reich, J. T. Marakovits, T. J. Prins, R. Zhou, J. Tikhe, E. S. Littlefield, T. M. Bleckman, M. B. Wallace, T. L. Little, C. E. Ford, J. W. Meador, 3rd, R. A. Ferre, E. L. Brown, S. L. Binford, D. M. DeLisle and S. T. Worland, *J. Med. Chem.*, 1998, **41**, 2819.

20 H. Yang, M. Yang, Y. Ding, Y. Liu, Z. Lou, Z. Zhou, L. Sun, L. Mo, S. Ye, H. Pang, G. F. Gao, K. Anand, M. Bartlam, R. Hilgenfeld and Z. Rao, *Proc. Natl. Acad. Sci. U. S. A.*, 2003, **100**, 13190.

21 P. S. Dragovich, R. Zhou, S. E. Webber, T. J. Prins, A. K. Kwok, K. Okano, S. A. Fuhrman, L. S. Zalman, F. C. Maldonado, E. L. Brown, J. W. Meador, 3rd, A. K. Patick, C. E. Ford, M. A. Brothers, S. L. Binford, D. A. Matthews, R. A. Ferre and S. T. Worland, *Bioorg. Med. Chem. Lett.*, 2000, **10**, 45.

22 M. A. Murray, J. W. Janc, S. Venkatraman and L. M. Babe, *Antivir. Chem. Chemother.*, 2001, **12**, 273.

23 M. O. Sydnes, Y. Hayashi, V. K. Sharma, T. Hamada, U. Bacha, J. Barrila, E. Freire and Y. Kiso, *Tetrahedron*, 2006, **62**, 8601.

24 S.-H. Chen, J. Lamar, F. Victor, N. Snyder, R. Johnson, B. A. Heinz, M. Wakulchik and Q. M. Wang, *Bioorg. Med. Chem. Lett.*, 2003, **13**, 3531.

25 M. A. van de Plassche, M. Barniol-Xicota and S. H. Verhelst, *ChemBioChem*, 2020, **21**, 3383.

26 C. P. Chuck, C. Chen, Z. Ke, D. C. Wan, H. F. Chow and K. B. Wong, *Eur. J. Med. Chem.*, 2013, **59**, 1.

27 S. E. Webber, K. Okano, T. L. Little, S. H. Reich, Y. Xin, S. A. Fuhrman, D. A. Matthews, R. A. Love, T. F. Hendrickson, A. K. Patick, J. W. Meador, 3rd, R. A. Ferre, E. L. Brown, C. E. Ford, S. L. Binford and S. T. Worland, *J. Med. Chem.*, 1998, **41**, 2786.

28 H. Z. Zhang, H. Zhang, W. Kemnitzer, B. Tseng, J. Cinatl, M. Michaelis, H. W. Doerr and S. X. Cai, *J. Med. Chem.*, 2006, **49**, 1198.

29 B. A. Malcolm, C. Lowe, S. Shechosky, R. T. McKay, C. C. Yang, V. J. Shah, R. J. Simon, J. C. Vederas and D. V. Santi, *Biochemistry*, 1995, **34**, 8172.

30 L. S. Deng, Z. Muhaxhiri, M. K. Estes, T. Palzkill, B. V. V. Prasad and Y. C. Song, *MedChemComm*, 2013, **4**, 1354.

31 T. S. Morris, S. Frermann, S. Shechosky, C. Lowe, M. S. Lall, V. Gauss-Muller, R. H. Purcell, S. U. Emerson, J. C. Vederas and B. A. Malcolm, *Bioorg. Med. Chem.*, 1997, **5**, 797.

32 T. Regnier, D. Sarma, K. Hidaka, U. Bacha, E. Freire, Y. Hayashi and Y. Kiso, *Bioorg. Med. Chem. Lett.*, 2009, **19**, 2722.

33 Y. K. Ramtohul, M. N. G. James and J. C. Vederas, *J. Org. Chem.*, 2002, **67**, 3169.

34 T. A. Shepherd, G. A. Cox, E. McKinney, J. Tang, M. Wakulchik, R. E. Zimmerman and E. C. Villarreal, *Bioorg. Med. Chem. Lett.*, 1996, **6**, 2893.

35 R. D. Hill and J. C. Vederas, *J. Org. Chem.*, 1999, **64**, 9538.

36 J. S. Kong, S. Venkatraman, K. Furness, S. Nimkar, T. A. Shepherd, Q. M. Wang, J. Aube and R. P. Hanzlik, *J. Med. Chem.*, 1998, **41**, 2579.

37 Y. M. Shao, W. B. Yang, T. H. Kuo, K. C. Tsai, C. H. Lin, A. S. Yang, P. H. Liang and C. H. Wong, *Bioorg. Med. Chem.*, 2008, **16**, 4652.

38 L. Li, B. C. Chenna, K. S. Yang, T. R. Cole, Z. T. Goodall, M. Giardini, Z. Moghadamchargari, E. A. Hernandez, J. Gomez, C. M. Calvet, J. A. Bernatchez, D. M. Mellott, J. Zhu, A. Rademacher, D. Thomas, L. R. Blankenship, A. Drelich, A. Laganowsky, C. K. Tseng, W. R. Liu, A. J. Wand, J. Cruz-Reyes, J. L. Siqueira-Neto and T. D. Meek, *J. Med. Chem.*, 2021, **64**, 11267.

39 J. Zhu, L. Li, A. Drelich, B. C. Chenna, D. M. Mellott, Z. W. Taylor, V. Tat, C. Z. Garcia, A. Katzfuss, C. K. Tseng and T. D. Meek, *Front. Chem.*, 2022, **10**, 867928.

40 D. H. Goetz, Y. Choe, E. Hansell, Y. T. Chen, M. McDowell, C. B. Jonsson, W. R. Roush, J. McKerrow and C. S. Craik, *Biochemistry*, 2007, **46**, 8744.

41 K. Akaji, H. Konno, H. Mitsui, K. Teruya, Y. Shimamoto, Y. Hattori, T. Ozaki, M. Kusunoki and A. Sanjoh, *J. Med. Chem.*, 2011, **54**, 7962.

42 K. Teruya, Y. Hattori, Y. Shimamoto, K. Kobayashi, A. Sanjoh, A. Nakagawa, E. Yamashita and K. Akaji, *Biopolymers*, 2016, **106**, 391.

43 Y. Shimamoto, Y. Hattori, K. Kobayashi, K. Teruya, A. Sanjoh, A. Nakagawa, E. Yamashita and K. Akaji, *Bioorg. Med. Chem.*, 2015, **23**, 876.

44 K. Ohnishi, Y. Hattori, K. Kobayashi and K. Akaji, *Bioorg. Med. Chem.*, 2019, **27**, 425.

45 S. Konno, P. Thanigaimalai, T. Yamamoto, K. Nakada, R. Kakiuchi, K. Takayama, Y. Yamazaki, F. Yakushiji, K. Akaji, Y. Kiso, Y. Kawasaki, S. E. Chen, E. Freire and Y. Hayashi, *Bioorg. Med. Chem.*, 2013, **21**, 412.

46 C. Proulx, D. Sabatino, R. Hopewell, J. Spiegel, Y. Garcia Ramos and W. D. Lubell, *Future Med. Chem.*, 2011, **3**, 1139.

47 J. McGrath and R. H. Abeles, *J. Med. Chem.*, 1992, **35**, 4279.

48 S. Venkatraman, J. S. Kong, S. Nimkar, Q. M. Wang, J. Aube and R. P. Hanzlik, *Bioorg. Med. Chem. Lett.*, 1999, **9**, 577.

49 W. M. Kati, H. L. Sham, J. O. McCall, D. A. Montgomery, G. T. Wang, W. Rosenbrook, L. Miesbauer, A. Buko and D. W. Norbeck, *Arch. Biochem. Biophys.*, 1999, **362**, 363.

50 H. L. Sham, W. Rosenbrook, W. Kati, D. A. Betebenner, N. E. Wideburg, A. Saldívar, J. J. Plattner and D. W. Norbeck, *J. Chem. Soc., Perkin Trans. 1*, 1995, 1081.

51 Y. T. Huang, B. A. Malcolm and J. C. Vederas, *Bioorg. Med. Chem.*, 1999, **7**, 607.



52 T. W. Lee, M. M. Cherney, C. Huitema, J. Liu, K. E. James, J. C. Powers, L. D. Eltis and M. N. James, *J. Mol. Biol.*, 2005, **353**, 1137.

53 T. W. Lee, M. M. Cherney, J. Liu, K. E. James, J. C. Powers, L. D. Eltis and M. N. James, *J. Mol. Biol.*, 2007, **366**, 916.

54 J. Breidenbach, C. Lemke, T. Pillaiyar, L. Schakel, G. Al Hamwi, M. Diett, R. Gedschold, N. Geiger, V. Lopez, S. Mirza, V. Namasivayam, A. C. Schiedel, K. Sylvester, D. Thimm, C. Vielmuth, L. Phuong Vu, M. Zyulina, J. Bodem, M. Gutschow and C. E. Muller, *Angew. Chem., Int. Ed.*, 2021, **60**, 10423.

55 C. Gilon, D. Halle, M. Chorev, Z. Selinger and G. Byk, *Biopolymers*, 1991, **31**, 745.

56 J. D. Tyndall and D. P. Fairlie, *Curr. Med. Chem.*, 2001, **8**, 893.

57 M. P. Glenn, L. K. Pattenden, R. C. Reid, D. P. Tyssen, J. D. Tyndall, C. J. Birch and D. P. Fairlie, *J. Med. Chem.*, 2002, **45**, 371.

58 C. J. White and A. K. Yudin, *Nat. Chem.*, 2011, **3**, 509.

59 E. Marsault and M. L. Peterson, *J. Med. Chem.*, 2011, **54**, 1961.

60 F. Giordanetto and J. Kihlberg, *J. Med. Chem.*, 2014, **57**, 278.

61 S. R. Mandadapu, P. M. Weerawarna, A. M. Prior, R. A. Uy, S. Aravapalli, K. R. Alliston, G. H. Lushington, Y. Kim, D. H. Hua, K. O. Chang and W. C. Groutas, *Bioorg. Med. Chem. Lett.*, 2013, **23**, 3709.

62 P. M. Weerawarna, Y. Kim, A. C. Galasiti Kankanamalage, V. C. Damalanka, G. H. Lushington, K. R. Alliston, N. Mehzabeen, K. P. Battaile, S. Lovell, K. O. Chang and W. C. Groutas, *Eur. J. Med. Chem.*, 2016, **119**, 300.

63 A. C. Galasiti Kankanamalage, P. M. Weerawarna, A. D. Rathnayake, Y. Kim, N. Mehzabeen, K. P. Battaile, S. Lovell, K. O. Chang and W. C. Groutas, *Proteins*, 2019, **87**, 579.

64 V. C. Damalanka, Y. Kim, A. C. Galasiti Kankanamalage, G. H. Lushington, N. Mehzabeen, K. P. Battaile, S. Lovell, K. O. Chang and W. C. Groutas, *Eur. J. Med. Chem.*, 2017, **127**, 41.

65 K. Namoto, F. Sirockin, H. Sellner, C. Wiesmann, F. Villard, R. J. Moreau, E. Valeur, S. C. Paulding, S. Schleeger, K. Schipp, J. Loup, L. Andrews, R. Swale, M. Robinson and C. J. Farady, *Bioorg. Med. Chem. Lett.*, 2018, **28**, 906.

66 P. S. Dragovich, T. J. Prins, R. Zhou, S. A. Fuhrman, A. K. Patick, D. A. Matthews, C. E. Ford, J. W. Meador, 3rd, R. A. Ferre and S. T. Worland, *J. Med. Chem.*, 1999, **42**, 1203.

67 P. S. Dragovich, T. J. Prins, R. Zhou, S. E. Webber, J. T. Marakovits, S. A. Fuhrman, A. K. Patick, D. A. Matthews, C. A. Lee and C. E. Ford, *J. Med. Chem.*, 1999, **42**, 1213.

68 R. P. Jain and J. C. Vedera, *Bioorg. Med. Chem. Lett.*, 2004, **14**, 3655.

69 C. J. Kuo, J. J. Shie, J. M. Fang, G. R. Yen, J. T. A. Hsu, H. G. Liu, S. N. Tseng, S. C. Chang, C. Y. Lee, S. R. Shih and P. H. Liang, *Bioorg. Med. Chem.*, 2008, **16**, 7388.

70 Y. Wang, B. Yang, Y. Zhai, Z. Yin, Y. Sun and Z. Rao, *Antimicrob. Agents Chemother.*, 2015, **59**, 2636.

71 Y. Wang, L. Cao, Y. Zhai, Z. Yin, Y. Sun and L. Shang, *Antimicrob. Agents Chemother.*, 2017, **61**, e00298.

72 Y. Y. Zhai, X. S. Zhao, Z. J. Cui, M. Wang, Y. X. Wang, L. F. Li, Q. Sun, X. Yang, D. B. Zeng, Y. Liu, Y. N. Sun, Z. Y. Lou, L. Q. Shang and Z. Yin, *J. Med. Chem.*, 2015, **58**, 9414.

73 D. Zeng, Y. Ma, R. Zhang, Q. Nie, Z. Cui, Y. Wang, L. Shang and Z. Yin, *Bioorg. Med. Chem. Lett.*, 2016, **26**, 1762.

74 Y. Y. Zhai, Y. Y. Ma, F. Ma, Q. D. Nie, X. J. Ren, Y. X. Wang, L. Q. Shang and Z. Yin, *Eur. J. Med. Chem.*, 2016, **124**, 559.

75 K. C. Tiew, G. He, S. Aravapalli, S. R. Mandadapu, M. R. Gunnam, K. R. Alliston, G. H. Lushington, Y. Kim, K. O. Chang and W. C. Groutas, *Bioorg. Med. Chem. Lett.*, 2011, **21**, 5315.

76 A. C. Galasiti Kankanamalage, Y. Kim, P. M. Weerawarna, R. A. Z. Uy, V. C. Damalanka, S. R. Mandadapu, K. R. Alliston, N. Mehzabeen, K. P. Battaile and S. Lovell, *J. Med. Chem.*, 2015, **58**, 3144.

77 A. D. Rathnayake, Y. Kim, C. S. Dampalla, H. N. Nguyen, A. M. Jesri, M. M. Kashipathy, G. H. Lushington, K. P. Battaile, S. Lovell, K. O. Chang and W. C. Groutas, *J. Med. Chem.*, 2020, **63**, 11945.

78 A. C. Galasiti Kankanamalage, Y. Kim, A. D. Rathnayake, K. R. Alliston, M. M. Butler, S. C. Cardinale, T. L. Bowlin, W. C. Groutas and K. O. Chang, *J. Med. Chem.*, 2017, **60**, 6239.

79 F. Amblard, S. M. Zhou, P. Liu, J. Yoon, B. Cox, K. Mazzarelli, B. D. Kuiper, L. C. Kovari and R. F. Schinazi, *Bioorg. Med. Chem. Lett.*, 2018, **28**, 2165.

80 R. P. Jain, H. I. Pettersson, J. Zhang, K. D. Aull, P. D. Fortin, C. Huitema, L. D. Eltis, J. C. Parrish, M. N. James and D. S. Wishart, *J. Med. Chem.*, 2004, **47**, 6113.

81 A. K. Ghosh, K. Xi, K. Ratia, B. D. Santarsiero, W. Fu, B. H. Harcourt, P. A. Rota, S. C. Baker, M. E. Johnson and A. D. Mesecar, *J. Med. Chem.*, 2005, **48**, 6767.

82 H. Yang, W. Xie, X. Xue, K. Yang, J. Ma, W. Liang, Q. Zhao, Z. Zhou, D. Pei, J. Ziebuhr, R. Hilgenfeld, K. Y. Yuen, L. Wong, G. Gao, S. Chen, Z. Chen, D. Ma, M. Bartlam and Z. Rao, *PLoS Biol.*, 2005, **3**, e324.

83 S. Yang, S. J. Chen, M. F. Hsu, J. D. Wu, C. T. Tseng, Y. F. Liu, H. C. Chen, C. W. Kuo, C. S. Wu, L. W. Chang, W. C. Chen, S. Y. Liao, T. Y. Chang, H. H. Hung, H. L. Shr, C. Y. Liu, Y. A. Huang, L. Y. Chang, J. C. Hsu, C. J. Peters, A. H. Wang and M. C. Hsu, *J. Med. Chem.*, 2006, **49**, 4971.

84 P. Thanigaimalai, S. Konno, T. Yamamoto, Y. Koiwai, A. Taguchi, K. Takayama, F. Yakushiji, K. Akaji, S. E. Chen, A. Naser-Tavakolian, A. Schon, E. Freire and Y. Hayashi, *Eur. J. Med. Chem.*, 2013, **68**, 372.

85 P. Thanigaimalai, S. Konno, T. Yamamoto, Y. Koiwai, A. Taguchi, K. Takayama, F. Yakushiji, K. Akaji, Y. Kiso, Y. Kawasaki, S. E. Chen, A. Naser-Tavakolian, A. Schon, E. Freire and Y. Hayashi, *Eur. J. Med. Chem.*, 2013, **65**, 436.

86 C. S. B. Chia, W. Xu and P. Shuyi Ng, *ChemMedChem*, 2022, **17**, e202100576.

87 K. Akaji, *Amino Acids Pept. Proteins*, 2017, 228.



88 T. Pillaiyar, M. Manickam, V. Namasivayam, Y. Hayashi and S. H. Jung, *J. Med. Chem.*, 2016, **59**, 6595.

89 T. Pillaiyar, L. L. Wendt, M. Manickam and M. Easwaran, *Med. Res. Rev.*, 2021, **41**, 72.

90 V. Kumar, J. S. Shin, J. J. Shie, K. B. Ku, C. Kim, Y. Y. Go, K. F. Huang, M. Kim and P. H. Liang, *Antiviral Res.*, 2017, **141**, 101.

91 A. C. G. Kankanamalage, Y. Kim, V. C. Damalanka, A. D. Rathnayake, A. R. Fehr, N. Mehzabeen, K. P. Battaile, S. Lovell, G. H. Lushington, S. Perlman, K. O. Chang and W. C. Groutas, *Eur. J. Med. Chem.*, 2018, **150**, 334.

92 L. Zhang, D. Lin, Y. Kusov, Y. Nian, Q. Ma, J. Wang, A. Von Brunn, P. Leyssen, K. Lanko and J. Neyts, *J. Med. Chem.*, 2020, **63**, 4562.

93 S. L. Binford, F. Maldonado, M. A. Brothers, P. T. Weady, L. S. Zalman, J. W. Meador, 3rd, D. A. Matthews and A. K. Patick, *Antimicrob. Agents Chemother.*, 2005, **49**, 619.

94 H. M. Wang and P. H. Liang, *Expert Opin. Ther. Pat.*, 2010, **20**, 59.

95 R. Ramajayam, K. P. Tan and P. H. Liang, *Biochem. Soc. Trans.*, 2011, **39**, 1371.

96 Y. Kim, S. Lovell, K. C. Tiew, S. R. Mandadapu, K. R. Alliston, K. P. Battaile, W. C. Groutas and K. O. Chang, *J. Virol.*, 2012, **86**, 11754.

97 J. Tan, K. H. Verschueren, K. Anand, J. Shen, M. Yang, Y. Xu, Z. Rao, J. Bigalke, B. Heisen, J. R. Mesters, K. Chen, X. Shen, H. Jiang and R. Hilgenfeld, *J. Mol. Biol.*, 2005, **354**, 25.

98 L. Zhang, D. Lin, X. Sun, U. Curth, C. Drosten, L. Sauerhering, S. Becker, K. Rox and R. Hilgenfeld, *Science*, 2020, **368**, 409.

99 B. Bai, A. Belovodskiy, M. Hena, A. S. Kandadai, M. A. Joyce, H. A. Saffran, J. A. Shields, M. B. Khan, E. Arutyunova, J. Lu, S. K. Bajwa, D. Hockman, C. Fischer, T. Lamer, W. Vuong, M. J. van Belkum, Z. Gu, F. Lin, Y. Du, J. Xu, M. Rahim, H. S. Young, J. C. Vederas, D. L. Tyrrell, M. J. Lemieux and J. A. Nieman, *J. Med. Chem.*, 2022, **65**, 2905.

100 S. Mondal, Y. Chen, G. J. Lockbaum, S. Sen, S. Chaudhuri, A. C. Reyes, J. M. Lee, A. N. Kaur, N. Sultana and M. D. Cameron, *J. Am. Chem. Soc.*, 2022, **144**, 21035.

101 W. Dai, B. Zhang, X. M. Jiang, H. Su, J. Li, Y. Zhao, X. Xie, Z. Jin, J. Peng, F. Liu, C. Li, Y. Li, F. Bai, H. Wang, X. Cheng, X. Cen, S. Hu, X. Yang, J. Wang, X. Liu, G. Xiao, H. Jiang, Z. Rao, L. K. Zhang, Y. Xu, H. Yang and H. Liu, *Science*, 2020, **368**, 1331.

102 J. Qiao, Y. S. Li, R. Zeng, F. L. Liu, R. H. Luo, C. Huang, Y. F. Wang, J. Zhang, B. Quan, C. Shen, X. Mao, X. Liu, W. Sun, W. Yang, X. Ni, K. Wang, L. Xu, Z. L. Duan, Q. C. Zou, H. L. Zhang, W. Qu, Y. H. Long, M. H. Li, R. C. Yang, X. Liu, J. You, Y. Zhou, R. Yao, W. P. Li, J. M. Liu, P. Chen, Y. Liu, G. F. Lin, X. Yang, J. Zou, L. Li, Y. Hu, G. W. Lu, W. M. Li, Y. Q. Wei, Y. T. Zheng, J. Lei and S. Yang, *Science*, 2021, **371**, 1374.

103 Z. Xia, M. Sacco, Y. Hu, C. Ma, X. Meng, F. Zhang, T. Szeto, Y. Xiang, Y. Chen and J. Wang, *ACS Pharmacol. Transl. Sci.*, 2021, **4**, 1408.

104 C. Lin, K. Lin, Y. P. Luong, B. G. Rao, Y. Y. Wei, D. L. Brennan, J. R. Fulghum, H. M. Hsiao, S. Ma, J. P. Maxwell, K. M. Cottrell, R. B. Perni, C. A. Gates and A. D. Kwong, *J. Biol. Chem.*, 2004, **279**, 17508.

105 S. Venkatraman, S. L. Bogen, A. Arasappan, F. Bennett, K. Chen, E. Jao, Y. T. Liu, R. Lovey, S. Hendrata, Y. Huang, W. Pan, T. Parekh, P. Pinto, V. Popov, R. Pike, S. Ruan, B. Santhanam, B. Vibulbhan, W. Wu, W. Yang, J. Kong, X. Liang, J. Wong, R. Liu, N. Butkiewicz, R. Chase, A. Hart, S. Agrawal, P. Ingravallo, J. Pichardo, R. Kong, B. Baroudy, B. Malcolm, Z. Guo, A. Prongay, V. Madison, L. Broske, X. Cui, K. C. Cheng, Y. Hsieh, J. M. Brisson, D. Prelusky, W. Korfomacher, R. White, S. Bogdanowich-Knipp, A. Pavlovsky, P. Bradley, A. K. Saksena, A. Ganguly, J. Piwinski, V. Girijavallabhan and F. G. Njoroge, *J. Med. Chem.*, 2006, **49**, 6074.

106 R. L. Hoffman, R. S. Kania, M. A. Brothers, J. F. Davies, R. A. Ferre, K. S. Gajiwala, M. He, R. J. Hogan, K. Kozminski, L. Y. Li, J. W. Lockner, J. Lou, M. T. Marra, L. J. Mitchell, Jr., B. W. Murray, J. A. Nieman, S. Noell, S. P. Planken, T. Rowe, K. Ryan, G. J. Smith, 3rd, J. E. Solowiej, C. M. Steppan and B. Taggart, *J. Med. Chem.*, 2020, **63**, 12725.

107 B. Boras, R. M. Jones, B. J. Anson, D. Arenson, L. Aschenbrenner, M. A. Bakowski, N. Beutler, J. Binder, E. Chen, H. Eng, H. Hammond, J. Hammond, R. E. Haupt, R. Hoffman, E. P. Kadar, R. Kania, E. Kimoto, M. G. Kirkpatrick, L. Lanyon, E. K. Lendy, J. R. Lillis, J. Logue, S. A. Luthra, C. Ma, S. W. Mason, M. E. McGrath, S. Noell, R. S. Obach, O. B. Mn, R. O'Connor, K. Ogilvie, D. Owen, M. Pettersson, M. R. Reese, T. F. Rogers, R. Rosales, M. I. Rossulek, J. G. Sathish, N. Shirai, C. Steppan, M. Ticehurst, L. W. Updyke, S. Weston, Y. Zhu, K. M. White, A. Garcia-Sastre, J. Wang, A. K. Chatterjee, A. D. Mesecar, M. B. Frieman, A. S. Anderson and C. Allerton, *Nat. Commun.*, 2021, **12**, 6055.

108 D. R. Owen, C. M. N. Allerton, A. S. Anderson, L. Aschenbrenner, M. Avery, S. Berritt, B. Boras, R. D. Cardin, A. Carlo, K. J. Coffman, A. Dantonio, L. Di, H. Eng, R. Ferre, K. S. Gajiwala, S. A. Gibson, S. E. Greasley, B. L. Hurst, E. P. Kadar, A. S. Kalgutkar, J. C. Lee, J. Lee, W. Liu, S. W. Mason, S. Noell, J. J. Novak, R. S. Obach, K. Ogilvie, N. C. Patel, M. Pettersson, D. K. Rai, M. R. Reese, M. F. Sammons, J. G. Sathish, R. S. P. Singh, C. M. Steppan, A. E. Stewart, J. B. Tuttle, L. Updyke, P. R. Verhoest, L. Wei, Q. Yang and Y. Zhu, *Science*, 2021, **374**, 1586.

109 H. Eng, A. L. Dantonio, E. P. Kadar, R. S. Obach, L. Di, J. Lin, N. C. Patel, B. Boras, G. S. Walker, J. J. Novak, E. Kimoto, R. S. P. Singh and A. S. Kalgutkar, *Drug Metab. Dispos.*, 2022, **50**, 576.

110 J. Hammond, H. Leister-Tebbe, A. Gardner, P. Abreu, W. Bao, W. Wisemandle, M. Baniecki, V. M. Hendrick, B. Damle, A. Simon-Campos, R. Pypstra, J. M. Rusnak and E.-H. Investigators, *N. Engl. J. Med.*, 2022, **386**, 1397.

